Molecular investigation of the structure-activity relationship of human Oligopeptide transporter 2 (PepT2) and polymyxin B

Jingchun Gao

Sydney Pharmacy School

Faculty of Medicine and Health

The University of Sydney

A thesis submitted to fulfill the requirements for the degree of

Master of Philosophy (Pharmacy)

Declaration

This graduation thesis titled "Molecular Investigation of the Structure-Activity Relationship of Human Oligopeptide Transporter 2 (PepT2) and Polymyxin B" is the result of my original research work conducted under the guidance and supervision of Fanfan Zhou, at the School of Pharmacy, University of Sydney.

This thesis represents my own efforts, thoughts, and conclusions derived from the experimental work carried out in the field of pharmaceutical sciences. All the sources of information, including but not limited to published and unpublished works of other researchers, have been duly acknowledged and appropriately referenced.

Jingchun Gao

June 2023

Acknowledgments

I would like to express my heartfelt gratitude to my supervisor, Dr. Fanfan Zhou, for her invaluable guidance and support throughout my research journey. Her expertise and patience have been instrumental in shaping this thesis. I am truly grateful for her mentorship.

I would also like to thank Janney Z. Quan Wang, a Ph.D. Candidate and member of our experimental group, for her collaboration and assistance. Her input and discussions have greatly improved the quality of our work, and I appreciate her contributions.

I would like to extend my thanks to Professor Jian Li from Monash University for providing us with MIPS-9541. His generosity in sharing this resource has allowed us to conduct essential experiments for our study. I am grateful for his expertise and willingness to collaborate.

I would like to acknowledge the support of my family and friends who have been there for me throughout this academic journey. Their encouragement and belief in me have been invaluable.

Lastly, I would like to thank the university staff and faculty for creating a conducive learning environment.

To all those who have directly or indirectly contributed to the completion of this thesis, I offer my sincere appreciation. Your support and guidance have been greatly appreciated.

Contents

List of Figures

List of Tables

Abstract

Polymyxins are a class of antibiotics known for their potent activity against multidrug-resistant Gram-negative bacteria; however, their clinical usage is greatly limited to due to their renal toxicity. The recent research has revealed the interaction between polymyxin and human Oligopeptide transporter 2 (hPepT2). It was found that hPepT2 may be responsible for the renal reabsorption of polymyxins, which may greatly contribute to the toxic accumulation of polymyxins in the kidney. Therefore, understanding the interaction between polymyxins and hPepT2 enables us to strategically manipulate their interaction and then inhibit the toxic accumulation of polymyxins in the kidney. And to establish the structure-interaction relationship model of polymyxins and hPepTs forms the basis of designing new polymyxin-like antibiotics that has reduced nephrotoxicity. This study examined several residues of hPepT2 for their involvement in its recognition of polymyxins and hPepT2-mediated cellular uptake of polymyxins through functional mutagenesis.

Polymyxin B is one of the two polymyxins used in clinical setting. Colistin is clinically offered in its prodrug format CMS, but polymyxin B is an active drug. CMS is not known as a substrate of PepTs. Thus polymyxin B is a better and representative probe in this study. Based on the preliminary prediction via computer modelling, 8 residues of hPepT2 have been proposed to be critical in polymyxin B recognition. Each of these residues were mutagenized to alanine. Alanine scanning mutagenesis is a widely

adopted method to study the SIR of membrane transporters. Alanine has the simplest side chain; changing a residue into alanine would reflect the most dramatic structural change of an amino acid. These single mutants were then investigated for their capability in mediating the cellular uptake of the classic substrate Glycyl-sarcosine (Gly-sar) and polymyxin B in overexpressing HEK 293 cells. Gly-sar is a protypical substrate of PepTs, which has been widely adopted for functional analysis of PepTs. MIPS-9541 is the customised fluorescence-conjugated polymyxin B1. This compound functions as a surrogate for polymyxin B, facilitating the investigation of polymyxin B uptake mechanisms. For those mutants with impaired transporter function, their kinetic parameters (Km and Vmax) were estimated to further explore the involvement of these residues in polymyxin recognition and capacity of polymyxin transport. A further attempt was made to evaluate the protein expression of hPepT2 mutants; however, the approach was shown to be invalid as there is no valid commercially available antibody of hPepT2. A potential solution has then been proposed with the construction of the C-terminal Flag tagged hPepT2 construct.

When compared to the wild type, several mutants showed altered uptake of either Gly-sar or polymyxin B. The 79A and 555A mutant has reduced uptake for polymyxin B but that of Gly-sar was not impacted. The 208A mutant had a significantly higher uptake of Gly-sar but reduced transport of polymyxin B. The 214A, 215A and 622A mutants have reduced uptake for both substrates. The 317A and 342A mutants exhibited decreased uptake of Gly-sar but that of MIPS-9541 was not changed.

Based on the kinetic results for Gly-sar, the Km values of mutants 208A, 214A, 215A, and 342A were not significantly different from the wild type [hPepT2 (39.64 ± 3.004 μM), 208A (42.00 ± 3.519 μM), 214A (44.37 ± 3.365 μM), 215A (42.59 ± 7.909 μM), and 342A (49.66 ± 5.908 μM)], indicating comparable substrate affinity for Gly-sar. However, the Vmax of mutant 208A [187.8 ± 6.948 pmol/(μg4min)] was increased, while the Vmax of the other mutants was reduced compared to that of wild type {hPepT2 [(148.8 ± 4.916 pmol/(μg4min)], 214A [100.4 ± 3.403 pmol/(μg4min)], 342A [88.26 ± 5.178 pmol/(μg4min)], and 215 [65.84 ± 5.857 pmol/(μg*4min)]}.

In terms of the Km and Vmax of polymyxin B, mutant 215A [Km: 96.56 ± 20.85μM, Vmax: 8610 ± 1363.0 pmol/(μg/4min)] showed significantly reduced affinity but increased turnover rate than the wild type [Km: 47.11 ± 11.89μM, Vmax: 4252 ± 652.9 pmol/(μg/4min)]. Mutant 214A [Km: 38.13 ± 12.93μM, Vmax: 3457 ± 671.0 pmol/(μg/4min)] had a similar affinity and a slightly decreased Vmax to the wild type. Mutant 555A [Km: 26.66 ± 6.99 μM, Vmax: 2376 ± 320.8 pmol/(μg/4min)] had a comparable affinity to the wild type but a significantly reduced Vmax. Future studies will evaluate the protein expression of these mutants.

In conclusion, this study investigated several residues of hPepT2 for their involvement in hPepT2-mediated polymyxin uptake. The residue 79, 208, 215, 555, and 622 are potentially involved in the recognition or determining the transport turnover rate of hPepT2 in the transport of polymyxins. These residues will be further investigated to

establish the structure-activity relationship between polymyxins and hPepT2, which may form the basis for the future chemical modification of polymyxins in order to reduce their nephrotoxicity.

Introduction

1. Introduction:

Antibiotic resistance has emerged as a formidable global health challenge in recent years [1], with gram-negative "superbugs," such as Pseudomonas aeruginosa, Acinetobacter baumannii, and Enterobacteriaceae, being major culprits [2]. The gravity of this challenge cannot be overstated, as it poses a significant threat to public health, food security, and development worldwide [3], leading to escalated healthcare expenses, extended hospital stays, and augmented mortality rates. An estimated 1.2 million people succumb to drug-resistant infections annually, and by 2050, approximately 28.3 million individuals could be propelled into extreme poverty due to antibiotic resistance [4]. Additionally, hospital-acquired infections in the United States and Europe alone result in a financial loss of 13.5 billion dollars annually [4].

Antibiotic resistance occurs naturally and is exacerbated by the misuse of antibiotics in both humans and animals. Large pharmaceutical corporations have opted to abandon the development of new antibiotics owing to scientific complexity and less profit potentials than drugs for chronic conditions and diseases [5]. While attempts are being made to develop novel antibiotics, the injudicious use of current antibiotics has hastened the progression of antibiotic resistance [6].

1.1 Polymyxin

Polymyxins are a class of cyclic non-ribosomal polypeptides first identified in the 1940s and produced by the Gram-positive spore-forming soil bacterium *Paenibacillus polymyxa* [7]. However, such old antibiotics have limited clinical applicatons due to their severe nephrotoxicity [8].

Polymyxins are decapeptide molecules characterized by a cyclic heptapeptide amide-linked loop, intrinsically linked with four or five non-proteogenic diaminobutyric acids (Dab) residues (Figure 1). The loop is positioned between the Dab residue at position 4 and the threonine residue at the C-terminal end. Positions 1, 5, 8, and 9 contain L-configuration Dab residues, with position 2 exhibiting a conserved hydrophilic L-threonine residue. Position 3 may have a D-serine residue or a D- or L-Dab residue, depending on the circumstance. In contrast, position 6 adopts a D-configuration, albeit with variation between phenylalanine and leucine. Position 7 contains several L-hydrophobic residues, such as leucine and valine. Position 10 mostly has a L-threonine residue and rarely a L-leucine residue. The N-terminal is mostly a fatty-acyl group. Similar to other antimicrobial peptides, the hydrophilic and lipophilic properties are critical for their antimicrobial activity [9].

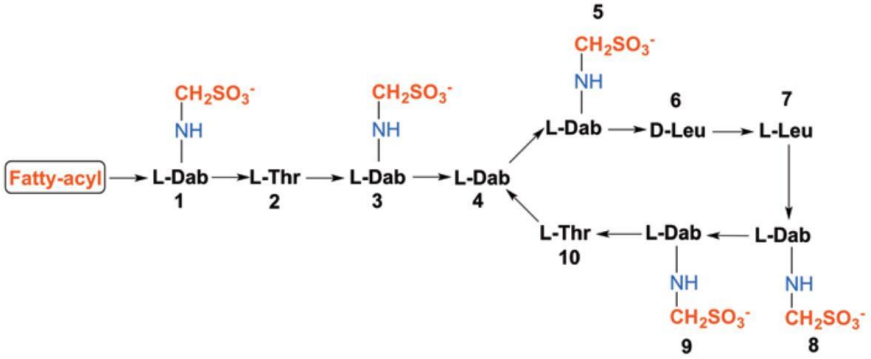

Fig. 1 Chemical structure of polymyxins

Polymyxin B and colistin (Polymyxin E) are the two primary clinically used polymyxin. These two antibiotics differ by a single residue at position 6, with polymyxin B containing a D-phenylalanine residue and colistin containing a D-leucine residue.

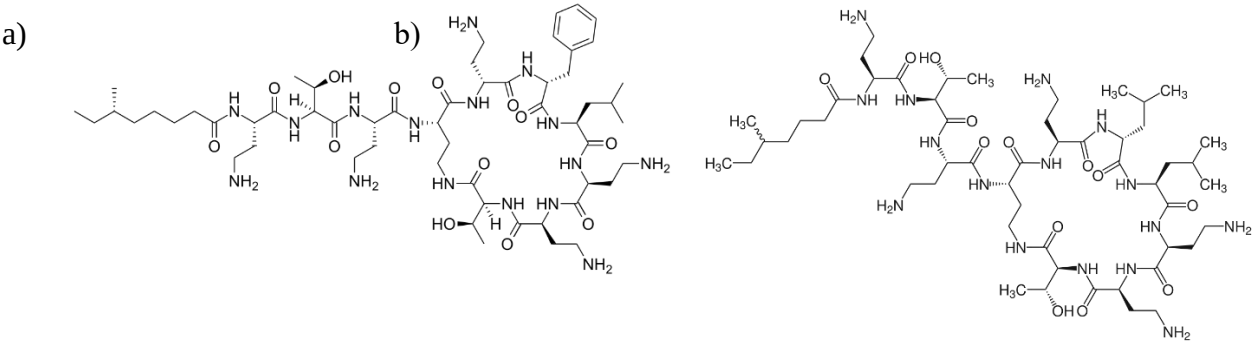

Fig. 2 Structure of (a) Polymyxin B and (b) Colistin

1.1.1 Clinical use of polymyxins

Bacterial biofilms are intricate communities of surface-attached bacteria linked by a self-produced glycoproteic matrix [10]. In cases where bacteria adhere to surfaces, such as prosthetic joints or the bronchial tree in cystic fibrosis, biofilm formation may ensue [11, 12]. This mechanism enables bacteria to survive exposure to clinical concentrations

of antibiotics. Previous research has demonstrated the efficacy of colistin in treating lung infections in cystic fibrosis patients caused by biofilms associated with Pseudomonas aeruginosa [13, 14]. Notably, recent research has demonstrated that using colistin as a monotherapy approach at clinical concentrations may lead to regrowth and the emergence of colistin-resistant P. aeruginosa biofilms [15]. In contrast, the adoption of combination therapy, such as administering high doses of colistin along with a secondary antibiotic, has demonstrated enhanced therapeutic outcomes [16]. Furthermore, the combination of colistin and ciprofloxacin or tobramycin has exhibited greater effectiveness than using each antibiotic alone, potentially attributed to their synergistic activity against the entire bacterial population within the biofilm [13, 17]. Colistin has also been administered via nebulization and intravenous routes, as well as through intracerebroventricular injection, to treat central nervous system and prosthetic joint infections [18]. However, clinical experience with colistin is limited due to its status as a last-line therapeutic option and uncertainty regarding its absolute safe and effective concentration.

Polymyxin B, akin to colistin, is utilized to treat infections arising from multidrug-resistant gram-negative bacteria [19]. However, there are apparent pharmacokinetic differences between polymyxin B and colistin, and as such, clinical data and experiments regarding polymyxin B cannot be directly correlated to colistin [20]. Currently, intravenous administration is the primary method of polymyxin B administration [21]. Although intramuscular injection is also feasible, this method

necessitates high doses of polymyxin B, which may lead to severe nephrotoxicity. Consequently, most studies do not employ intramuscular injections. As with colistin, the safe and effective mode and dosage of administration for polymyxin B could not be determined, owing to the small sample sizes and severity of infections in the patients.

1.1.2 Mode of action of polymyxins

The antimicrobial activity of polymyxins is well-established and involves the permeabilization of the outer membrane via direct interaction with lipopolysaccharide (LPS). This process begins with the electrostatic attraction of positively charged polymyxins to the negatively charged LPS, allowing for the N-terminal fatty acyl chain and position 6,7 of polymyxins to insert into the fatty acyl chain layer of the lipid A molecules (refer to Figure 1) [22]. This results in the expansion of the outer membrane due to the hydrophobic properties of polymyxin [23], followed by disruption of the physical integrity of the phospholipid bilayer of the inner membrane leaflet, ultimately leading to bacterial death [24].

However, recent research has demonstrated that the outer membrane may not be the sole target of polymyxin [25] and that other secondary mechanisms of action may exist, such as inhibiting bacterial respiration or generating reactive oxygen species [26, 27]. Furthermore, it has been suggested that colistin may exert its bactericidal activity by targeting LPS in the cytoplasmic membrane [28].

1.1.3 polymyxin-induced nephrotoxicity

To investigate the potential nephrotoxicity induced by polymyxin B and colistin, the urinary recovery of the administered dose was less than 1% after intravenous drug administration to rats [29]. This suggests that the reabsorption of polymyxin B and colistin occurs in rats' renal tubules, as its renal clearance is much lower than the anticipated glomerular filtration clearance [30]. Moreover, it has been indicated that polymyxin B and colistin primarily accumulate in the renal cortex, particularly in the renal proximal tubular cells, following intravenous administration [31, 32]. Analogously, upon subcutaneous administration of polymyxin B and colistin, renal cortex accumulation was observed, whereas no accumulation was detected in the lungs, liver, or heart [31]. The uptake of polymyxin B and colistin by renal tubular cells is partially mediated by megalin, a critical endocytic receptor responsible for the reabsorption of small bioactive molecules and proteins in glomerular filtrate [33], which has also been demonstrated to be competitively inhibited by polymyxin B and colistin concerning cytochrome c, a known megalin substrate [34, 35]. More importantly, the previous study demonstrated that human oligopeptide transporter (hPepT2) mediates the reabsorption of polymyxin B and colistin [36].

1.2 Oligopeptide transporters

Oligopeptides are a group of peptides consisting of 2 to 20 amino acids, while polypeptides encompass those containing more than 20 amino acids [37]. Oligopeptide transporters (PepTs), also known as Proton-coupled Oligopeptide Transporters (POTs), are integral membrane proteins that facilitate the transportation of various dipeptides, tripeptides, and peptide-like drugs across biological membranes [38]. POTs are composed of four isoforms, namely PepT1 (SLC15A1), PepT2 (SLC15A2), PhT1 (SLC15A4), and PhT2 (SLC15A3). The earliest investigations of oligopeptide transporters were conducted on brush border membrane vesicles (BBMV) [39]. In these studies, Ganapathy et al. discovered a unique transport system for dipeptides, tripeptides, and peptide-like drugs in renal tubular cells, which was stimulated by the H+ gradient [39, 40]. A decade later, Hediger et al. employed expression cloning techniques to identify the molecular basis of peptide transporters in mammals and assessed the functional characterization of Slc15a1-encoded PepT1 from a rabbit intestinal cDNA library [41]. Using $PepT_{St}$ isolated from *Streptococcus Thermophilus*, four dipeptides (Ala-Leu, Phe-Ala, Ala-Gln, and Asp-Glu) were discovered to bind to PepTst with high affinity [42]. Furthermore, $PepT_{St}$ can adapt to various peptide side chains by repositioning binding site residues and water molecules, thereby promoting a better fit [42]. This finding presented an additional avenue for exploring the properties of human PepTs.

1.2.1 Tissue localization of PepTs

The physiological and pharmacological properties of oligopeptide transporters in the human body largely depend on their location. In the digestive system, PepT1, a member of the SLC15 family, is predominantly expressed on the apical membrane of the human duodenum and ileum [43], facilitating the absorption of dipeptides and tripeptides from dietary protein and gastrointestinal secretions. PepT2 is primarily found in the glial cells of intestinal tissue, and it remains unclear whether PepT2-mediated uptake extends to the deep neuromuscular layer [44]. Studies utilizing western blot and immunohistochemical analysis have confirmed the expression of human PhT1 in the small intestinal villus epithelium for the first time [45]. A literature also reported the expression of PepTs in the eye and lung [46]. In the kidney, PepT1 is expressed in the anterior portion of the proximal convoluted tubule. In contrast, PepT2 is described in the posterior portion of the proximal convoluted tubule, with no expression of PepTs observed in other parts of the nephron [47]. During reabsorption, PepT1 and PepT2 collaborate to absorb peptide-bound amino acids effectively. The cerebral cortex, olfactory bulb, basal ganglia, cerebellum, and hindbrain slices of the adult brain exhibit PepT2 protein expression, with the highest level observed in the cerebral cortex, as determined by immunoblot and immunocytochemistry analyses [48]. PepT2 contributes to the clearance of neuropeptides, peptide fragments, and peptide-like drugs from cerebrospinal fluid, thereby regulating neuropeptide homeostasis in the extracellular fluid.

1.2.2 Substrate spectrum of PepTs

The transporters PepT1 and PepT2 play crucial roles in the human body by facilitating the absorption of dipeptides and tripeptides and serving as critical binding targets for numerous peptide drugs. Numerous distinctions exist in the substrate profiles of PepT1 and PepT2, potentially attributed to variations in their respective affinities.

PepT1, which is a low-affinity and high-capacity transporter, recognizes a range of drugs such as renin inhibitors [49], ACE inhibitors [50, 51], beta-lactam antibiotics [52], thrombin inhibitors [53], as well as acyclovir, ganciclovir, and levodopa Bar's amino acid prodrugs [54, 55]. PepT1 binds to most dipeptides and tripeptides consisting of L-form amino acids, except for tetrapeptides. Cephalexin and lorakatide exist as D- and L-enantiomers, and stereoselective uptake of these drugs by PepT1 has been observed, with the L-enantiomer demonstrating a greater affinity than the D-enantiomer [56]. Recent studies have shed light on the effect of peptide bonds on substrate uptake by PepT1. For instance, Brandsch et al. has reported that the presence of the peptide bond oxygen atom can be replaced by a sulphur modification of AlaPro, denoted as Ala-Ψ[CS-N]-Pro, without impeding PepT1 transport [57]. Additionally, PepT1 can transport substrates such as delta-aminolevulinic acid, valacyclovir, and valganciclovir, which lack peptide bonds [54, 58, 59]. PepT1 has also been shown to selectively transport dipeptides with trans conformation while disregarding dipeptides with cis conformation [60]. Furthermore, Meredith et al. have demonstrated the essentiality of the free amino terminus in binding affinity by finding that N-terminal acetylation of the

dipeptide Phe-Tyr 5 significantly reduces binding affinity [61]. Previous studies have identified large hydrophobic regions and C-terminal proline residues as key structural features associated with the most potent substrates and inhibitors of the PepT1 transporter [62, 63]. Additionally, greater lipophilicity has been demonstrated to enhance substrate affinity, while proline binding at the C-terminus increases affinity, as reported in recent studies [64, 65].

PepT2 is classified as a high-affinity, low-capacity transporter capable of transporting over 400 dipeptides and 8,000 tripeptides, consisting of 20 essential L-α-amino acids and the majority of D-enantiomers [66]. Apart from peptides, PepT2 exhibits recognition for various drugs such as amino cephalosporins, ACE inhibitors, and novel prodrugs [67-69]. The histidine residue of PepT2 indicates an interaction with the α-amino group, which suggests its possible involvement in substrate recognition by the peptide transporter. While a free α-amino group can significantly enhance substrate affinity to PepT2, studies have shown that it may not be necessary for recognition [70, 71]. The presence or absence of peptide bonds has no significant effect on the affinity between substrate and transporter. The ketomethylene group, a PepT2 substrate, can replace the peptide bond of aminolevulinic acid (ALA) [59]. Entranine, containing an N-terminal β-amino acid, has been observed to display an unusual binding affinity for PepT2. Additionally, research indicates that the hydrophobicity of the N-terminal region of aminopenicillin can contribute to an increase in binding affinity for PepT2 [59, 72]. The presence of acidic amino acids can lead to a significant reduction in

affinity compared to the same amino acid's presence at the C-terminus [73]. Introducing a single carbonyl group into the main chain can increase the compound's affinity and transport current by over 30 times [74]. Substrate affinity is mainly determined by the presence of hydrophobic side chains [75]. Several studies have provided evidence that incorporating a sizeable aromatic hydrophobic group in the dipeptide's N-terminal amino acid side chain can notably augment the binding affinity of various derivatives for PepT2 [67].

1.2.3 Transport mechanism of PepTs

The functions of PepT transporters exhibit similarities despite differences in their respective mechanisms of action, with regional differences in the site of action. Specifically, PepT1 primarily functions in the absorption of the small intestine epithelium, while PepT2 primarily functions in the reabsorption of nephron.

In the human body, PepT1 and PepT2 facilitate the transportation of dipeptides and tripeptides together with protons, as shown in Figure 3. These transporters' activity relies on an electrochemical proton gradient, where protons and Na+ ions are exchanged. Notably, the movement of Na+ and K+ ATPase influences the ion exchange rate [76]. Once dipeptides and tripeptides enter enterocytes or nephrons, they undergo hydrolysis in the cytosol. Various basolateral membrane amino acid transporters transport the resulting free amino acids into the bloodstream [76].

A recent study has reported the involvement of Ca^{2+} in the mechanism of the PepT1 transporter [77]. Upon absorption, dipeptides and tripeptides stimulate the calcium-sensing receptor (CaSR) situated on the basolateral membrane of enterocytes. This, in turn, leads to the activation of phospholipase C (PLC), resulting in the increased activation of the Ca2+-activated K+ channel (IKCa) and higher intracellular calcium concentrations ([Ca2+]cyt). Activation of IKCa channels facilitates K+ ion influx, inducing cell hyperpolarisation, which provides the driving force for the transepithelial uptake of dipeptides and tripeptides via PepT1.

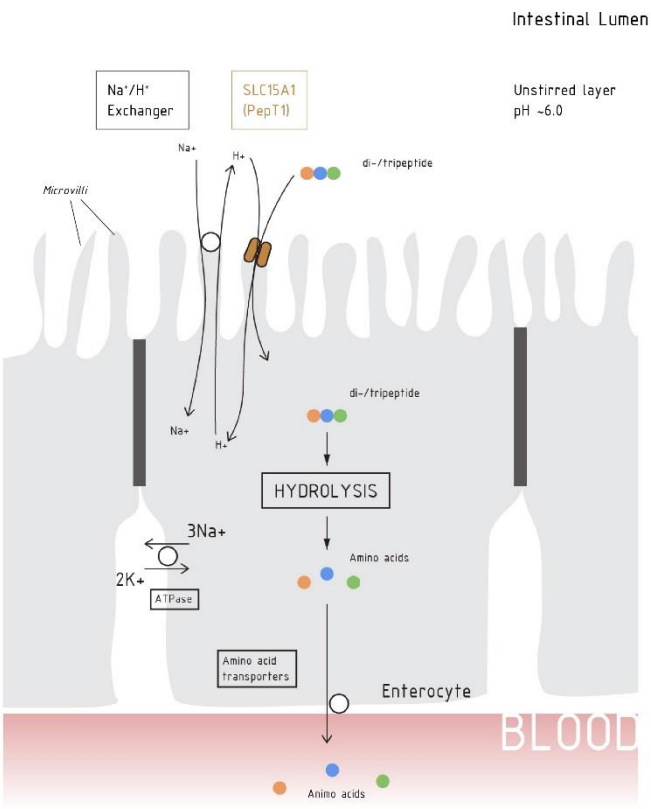

Fig. 3 Transport mechanism of PepTs in epithelial cells

1.2.4 Topology model of PepTs

The literature has proposed a topological model of PepTs, which predicts that PepTs have 12 transmembrane domains (TMDs) and an extracellular loop between TMDs 9 and 10 (Fig 4) [78, 79].

According to previous research, the entirety of the protein structure of PepT1, from the N-terminus to transmembrane domain 9 (TMD9), plays a significant role in determining all of its phenotypic traits [80]. Specifically, the first six TMDs define the pH dependence and form the substrate binding pocket's central region for PepTs [81]. In contrast, the transmembrane domains (TMDs) 7-9 have been suggested to play a significant role in determining substrate affinity [78]. The TMDs located at the N-terminus of PepTs have been found to adopt a pore-like structure, while TMDs 7-9 constitute a substrate-binding pocket. Previous research has indicated that residues 1-59 within the substrate binding domain can obstruct the side chain of dipeptides and the region between TMD 2 and 3, whereas residues 60-91 have been found to exert a notable influence on the pH sensitivity of PepTs [82]. Several residues essential for transport function have been identified through mutagenesis studies, including His57 in TMD 2, which is associated with proton binding, and His121, which is involved in substrate recognition [83]. Trp294, Glu595, and Tyr167 in TMDs 1, 3, 5, and 7 have also been shown to regulate substrate binding [84].

In PepT2, Tyr56, Tyr64, His121, Arg57, and Tyr167 have been proven critical for transporter activity and substrate binding [79]. The substrate binding domain in PepT2 has been shown to be in TMDs 7-9, and its phenotypic identity is determined by TMDs 1-9, with the centers of TMDs 2 and 3 likely contributing to its pH dependence. The functional divergence in the hydrophobic region of PepT2 has been shown to be critically dependent on amino acids within TMD 9-10 [85]. However, it is unlikely that the large extracellular loop situated between TMD 9 and 10 is involved in substrate binding [82].

N-glycosylation is a unique post-translational modification that occurs in eukaryotes and affects transporter properties and bioactivities by modifying appropriate asparagine residues of proteins with oligosaccharide structures [86]. Many studies have confirmed that N-glycosylation is essential for SLC transporters' localization, stability, and substrate binding [87, 88]. Glycosylation of intestinal PepT1 accounts for one-third of its total mass and shows a difference between the small intestine and the distal colon [89]. Alanine scanning mutagenesis has demonstrated that N-glycosylation is crucial for PepT1 transporter activity [90], and mutations on N50 residues have led to the decreased affinity of PepT1 with Gly-sar [91]. Moreover, N-glycosylation of PepT1 is resistant to proteolytic cleavage of proteinase K and intrinsically stable against trypsin [91].

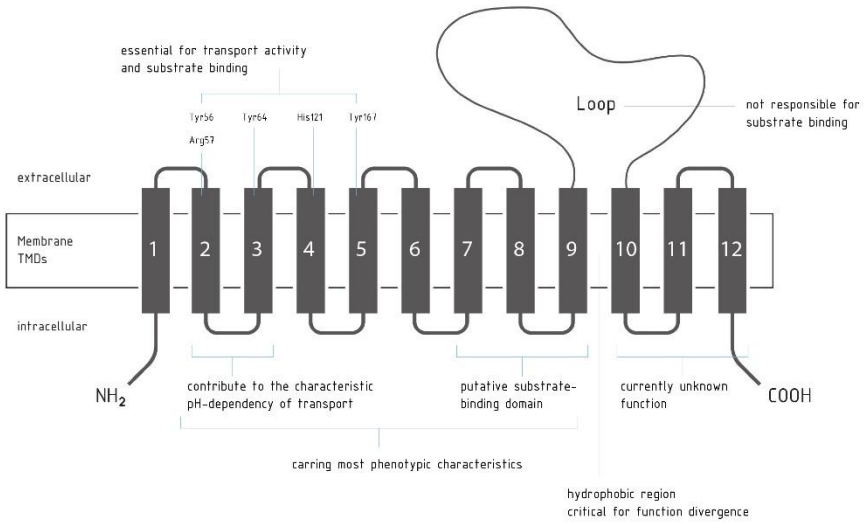

Fig. 4 Topology model of PepTs

1.2.5 Structure biology of PepTs

Although the crystal structure of PepTs has yet to be fully resolved, investigations of bacterial homologs of PepT1 and PepT2 have been conducted. $PepT_{so}$ was initially identified in *Shewanella oneidensis* [92], with subsequent examinations of the structures of $PepT_{St}$ from *Streptococcus thermophilus* [93], GkPOT from *Geobacillus kaustophilus* [94], $PepT_{so2}$ from *Shewanella oneidensis* [95], YePepT from *Yersinia enterocolitica* [96] and $PepT_{Xc}$ from *Xanthomonas campestris* [97]. These studies have revealed several standard structural features, including the canonical major facilitator superfamily (MFS) fold with 14 transmembrane helices [92-97]. The PepT transporter features a "V" shaped structure of two six-helix bundles at the N- and C-terminals. Helices H1-H6 and H7-H12 constitute the N- and C-terminals, respectively. Furthermore, it should be noted that two extra transmembrane helices, namely HA and HB, are conventionally incorporated into the cytoplasmic loop that connects the N-terminal and C-terminal bundles. However, their precise functional relevance has yet to be elucidated.

It has been suggested that the opening and closing of PepTs involve a hinge-like movement occurring at the apex of the H10–H11 [93]. Furthermore, the binding orientation of human PepTs to dipeptides is thought to be horizontal, while tripeptides may be oriented vertically [98]. However, a recent study demonstrated that the tripeptide binds to PepTs in a lateral manner similar to the dipeptide [99]. In addition, the side chain-binding pocket is relatively flexible due to conformational changes [99],

which presents a significant challenge for the structure-based design of drugs targeting PepTs.

The investigation of GKPOT sheds light on the mechanism of H+-coupled peptide symport for the POT family [94]. Specifically, the deprotonation of Glu310 upon binding with the carboxyl group of peptide substrates may trigger the intracellular release of substrates. At the same time, a salt bridge may simultaneously form between Glu310 and Arg43 to induce the conformational change of the transporter. Similarly, another study examining the proton coupling mechanism of PepTs obtained similar results, indicating that proton-bound transporters on the extracellular side facilitate the transition from inward- to outward-facing states [97].

To date, only one study has explored the function of the extracellular domain (ECD) of PepTs, which found that the interaction between trypsin and the ECD may improve substrate uptake efficiency [100].

A recent study has reported the cryogenic electron microscopy structures of human PepT1 and PepT2, uncovering discrepancies in their substrate recognition and transportation mechanisms [101]. As members of the Major Facilitator Superfamily (MFS), PepTs comprise 12 transmembrane (TM) helices and a bundle bridge linking both helical bundles. Regrettably, due to the low density of purified PepTs, the C-terminus of PepT1's last 25 residues, as well as the N-terminus and C-terminus of

PepT2's first 40 and last residues, respectively, could not be established, making them the first and only human PepT architectures. Also, no more Ha and Hb additional TMs were found in bacterial homologs in PepTs [101]. The study discovered novel sites of action compared to previous bacterial homologs, where the N-bundle of PepT1 and PepT2 exhibit more flexibility and dynamics, whereas the C-bundle exhibits greater rigidity. This contrasts with bacterial PepTs, where the N-terminal is the most rigid part of the transporter [95, 98, 102]. One possible explanation for this phenomenon could be attributed to an additional extracellular region between TM9 and TM10 in PepT1 and PepT2, which may necessitate the stabilizing function of the C-bundle.

The cryogenic electron microscopy structures proposed a hypothesis for the substrate transport mechanism in PepTs [101]. The hPepTs are initially outward facing the extracellular side, stabilized by two salt bridges. During peptide binding, the substrates are lodged in the charged central cavity, causing the bending of the N-bundle, which tightens the central cavity's binding. The transporter then switches to an inward state, stabilized by one salt bridge from two different sites. Finally, TM4 and TM5 separate from TM10 and TM11, causing the cytosolic side to open, leading to the loss of interaction between the substrate and amino acid, allowing the substrate to release into the cytoplasm.

1.3 Computer modelling of PepT2 and polymyxins (Unpublished)

The final objective of the entire research is to develop a polymyxin derivative that retains its high antibacterial efficacy while reduced nephrotoxicity. This requires identifying the critical residues of hPepT2 forming the binding pocket for polymyxins. The researchers at Monash University utilized a computer model to investigate the translocation of polymyxin B1 to the central binding pocket of $PepT2_{Xc}$, as shown in Figure 5 and 6. Given the unavailability of the actual structure of hPepT2, an analogue in bacteria was selected for analysis. The critical motifs responsible for the interactions between polymyxin B1 and PepT2Xc were identified, and the essential residues necessary for polymyxin binding in hPepT2 were subsequently validated in this project. Such findings hold promising implications for reducing the renal reabsorption of polymyxins, mitigating toxic accumulation, and increasing their clinical utility with minimized adverse effects.

The research related to this thesis only focuses on the phase 2 of the overall project. The current study aims to assess the role of the above-mentioned residues in polymyxin binding. Accordingly, the transporter mutagenesis data will contribute to establishing the structure-interaction model of hPepT2 and polymyxins. Following that, our collaborative team will customize and synthesize new polymyxin analogues that are optimally interact with hPepT2 (phase 3). Subsequently, Phase 4 study will comprehensively evaluate the pre-clinical characteristics of the newly synthesized polymyxin analogues.

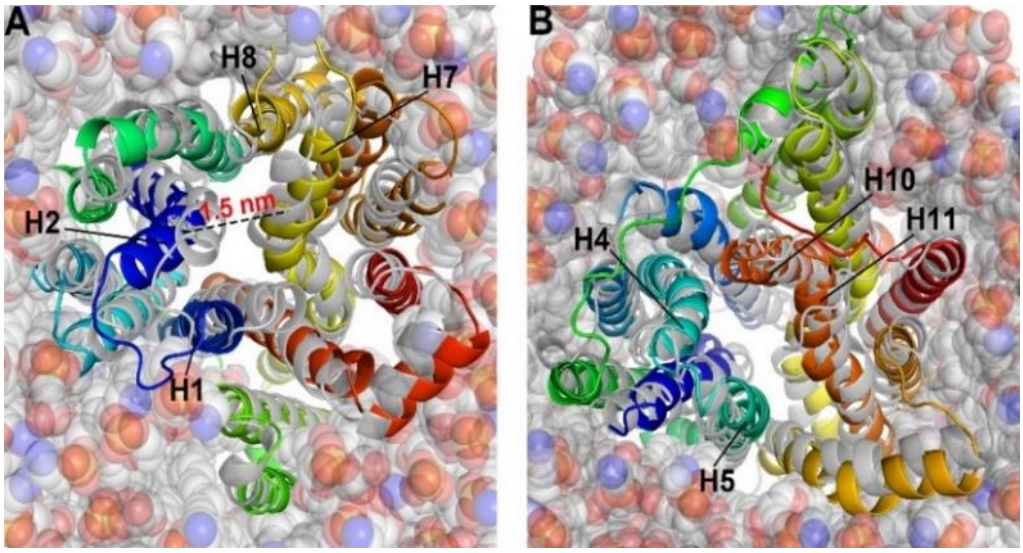

Fig. 5 The results of 1,000-ns MD simulations on PepT2Xc in human kidney tubular cell membrane revealed conformational transitions, as shown in both extracellular and intracellular side views (A and B). The key helices regulating these transitions are indicated in the label above.

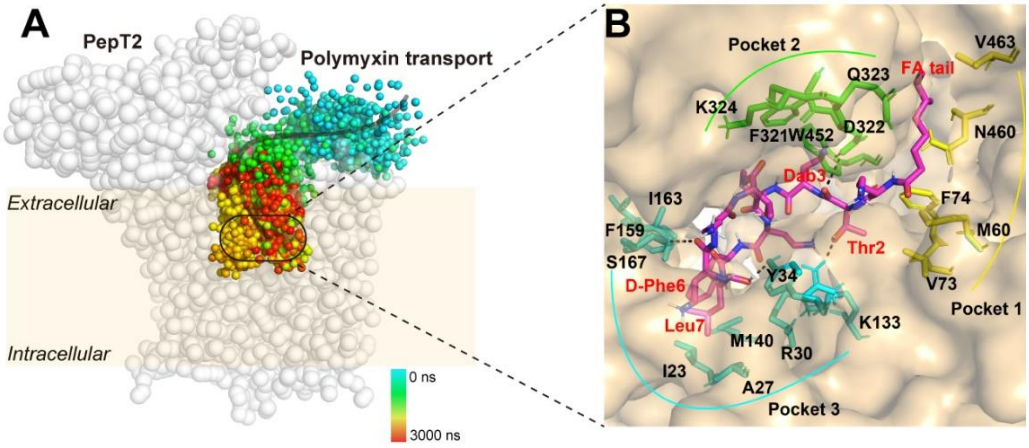

Fig. 6 (A) The translocation of polymyxin B1 to the central binding pocket of PepT2Xc was observed. (B) The motifs that were found to play a vital role in the interaction between polymyxin B1 and PepT2Xc were identified.

Materials and methods

2. Materials and methods

2.1 Materials

[^{3}H]-glycyl-sarcosine (Gly-Sar; 2.8Ci/mM)was purchased from Moravek. MIPS-9541 (FADDI-043, 5.24 mg) was generously provided by Professor Jian Li (University of Monash, Australia). Polymyxin B (6000IU/mg) was purchased from Glentham Life Sciences (ChemSupply, Australia). All additional chemicals were purchased from Sigma-Aldrich (Castle Hill, NSW, Australia).

The plasmid containing the coding regions of human PepT2 was purchased from Australian Biosearch (Balcatta, WA, Australia).

2.2 Site-directed mutagenesis

Mutagenic oligonucleotide primers were designed for single nucleotide mutations of Site-directed mutagenesis, as presented in Table 1. The principles of primer design included: 1) maintaining a primer length between 25 and 45 bases, 2) ensuring a melting temperature of ≥78°C using the formula Tm = 81.5 + 0.41(%GC) − (675/N) − % mismatch, where N denotes the primer length in bases and % values are whole numbers, 3) placing the target mutation residues in the middle of the primer sequence with approximately 10-15 bases of correct sequence on either side, 4) ensuring a minimum GC content of 40%, and 5) incorporating one or more C or G bases at the terminus. The

Phusion™ Site-Directed Mutagenesis Kit (Thermofisher) was utilized to create the PCR products. The PCR reaction was performed using Applied Biosystems 2720 Thermal Cycler, with the temperatures and times in Table 2.

The transformation was carried out using competent cells obtained from Promega, Australia. Lysogeny broth medium, comprising 10g Tryptone, 5g Yeast Extract, and 5g NaCl per liter, was supplemented with 0.1 mg/ml Ampicillin for bacterial culture, while agar plates containing 1.5% agar in LB medium were used for solid-phase bacterial culture. Purification of plasmid DNA from competent cells was performed using NanoDrop 1000 spectrophotometer (Thermo Scientific), while the concentration of the purified plasmid DNA was determined using GenElute™ HP Plasmid Miniprep Kit (Castle Hill, NSW, Australia). The presence of mutations in target residues of DNAs and the absence of undesired mutations were determined using BigDye Terminator v3.1 (Ramaciotti Centre for Genomics, University of New South Wales, Australia; data not displayed), ensuring accuracy and specificity.

2.3 Transfection in Hek293 cells

Hek293 cells were seeded on the 48-well cell culture plate coated with 0.1 mg/mL Poly-D-Lysine. The cell seeding density was 1.7×10^5 cells per well. The cells were incubated in a humidified atmosphere at 37°C and 5% CO2 in Dulbecco's modified Eagle's medium, which was supplemented with 10% fetal bovine serum (French Origin,

Bovogen) and 1% Gibco™ L-Glutamine (Invitrogen, U.S.A) to support their growth and maintenance. Following a 24-hour incubation period, Hek293 cells were transfected with either the previously mutated plasmid DNA or the pCI vector as a blank control, using Lipofectamine 2000 reagent (Invitrogen, Australia). After a further 24 hours had elapsed, the transport activity of cells was measured.

2.4 Transporter uptake assay

To evaluate the influx of prototypical substrates mediated by the transporter, the influx in control cells transfected with the vector was subtracted from the influx measured as the accumulation of radiolabelled compounds in cells overexpressing the transporter construct. Cellular uptake of a radiolabelled hPepT2 substrate was initiated at room temperature using pH 5 phosphate-buffered saline (PBS). For pH 7.4 PBS, the composition included 154 mM sodium chloride, 3.0 mM sodium phosphate dibasic, 1.1 mM potassium phosphate monobasic, and 1.0 mM each of magnesium chloride and calcium chloride. The total substrate concentration in uptake was 1.1 μM [^{3}H]Gly-Sar. The uptake duration was determined to be 6 minutes based on a previous pilot experiment [36]. After 6 minutes, the uptake process was terminated by rapidly washing the cells twice with cold pH 7 PBS, placed on ice, followed by cell lysis using 0.2 M NaOH and neutralization with 0.2 M HCl. The resulting solutions were collected in test tubes for liquid scintillation counting (Tri-Carb A4810TR, Mulgrave, VIC, Australia). The uptake count was normalized to the protein content in each well. The background

counts of cells transfected with vector pCI were subtracted from all uptake counts. The physiological state of the cells remained unchanged, as evidenced by no discernible difference in the accumulation of typical substrate Gly-sar between vector-transfected and parental cells under current experimental conditions (data not displayed). The data were presented as the mean ± SEM. The experiments were independently conducted three times with three replicates for each condition.

2.5 Western blot

Due to the inability of the hPepT2 antibody to detect the transporter protein, a C-terminal Flag-tagged hPepT2 construct was utilized for conducting protein assays. Incorporating Flag Tag, an artificial antigen with specific and high-affinity monoclonal antibodies, facilitated this process. Subsequently, a new set of transporter mutants were generated using the hPepT2-c-Flag plasmid as a template. The experimental methodology and reagent usage remain consistent with previous procedures. The presence of mutations in target residues of DNAs and the absence of undesired mutations were determined using BigDye Terminator v3.1, ensuring accuracy and specificity.

Hek293 cells were cultured at a density of 3.4 x105 cells per well on 24-well plates and transfected with mutant hPepT2-c-Flag plasmid DNA. Subsequently, the cells were detached using 1X Trypsin EDTA (0.5 g porcine trypsin and 0.2 g EDTA), washed with

PBS, and lysed using a lysis buffer [1% Nonidet P-40, 150 mM NaCl, 50mM Tris-HCl (pH 8), 2mM EDTA] containing a 1mM protease inhibitor. The cell-lysate mixture was allowed to incubate at room temperature for 30 minutes before being centrifuged at 12,000 rpm for 10 min, 4 ℃. The supernatant was collected and mixed with 10 µl of 5X Laemmli sample buffer (Bio-RAD).

The resulting samples were loaded onto 7.5% gels (composed of dH2O 21.9 ml, 3M pH 8.8 Tris 10ml, 40% Acry 7.5ml, 10 % SDS 400ul, 0.1 g/ml APS 200ul, TEMED 60ul) and subsequently transferred onto hydrophilic polyvinylidene fluoride membranes. The membranes were blocked with 5% (w/v) skim milk powder in PBST buffer for 1 hour at room temperature with shaking, followed by overnight incubation with primary antibodies at 4°C. The anti-flag rabbit primary antibody (1:1000) was employed. After washing with PBST buffer, the membranes were incubated with anti-rabbit secondary antibody (1:5000) for 1 hour at room temperature. Protein bands were detected using ECL reagents and visualized using ImageQuant LAS 500(Avantor®, PA, USA). The expression of the wild type hPepT2 in the total cell was determined.

2.6 MIPS-9541 uptake

The fluorescently labelled polymyxin substrate MIPS-9541 was used to conduct the functional transporter assay. This probe retains the pharmacophore of the polymyxins and maintains their pharmacological effect. MIPS-9541 is a novel fluorescent probe

with polymyxin's antibacterial and pharmacological impact [103, 104]. A previous study revealed that MIPS-9541 is a potent substrate of PepT2. The Km value of MIPS-9541 of hPepT2 was similar to that of glycyl-sarcosine, which is a typical substrate of hPepT2 [36].

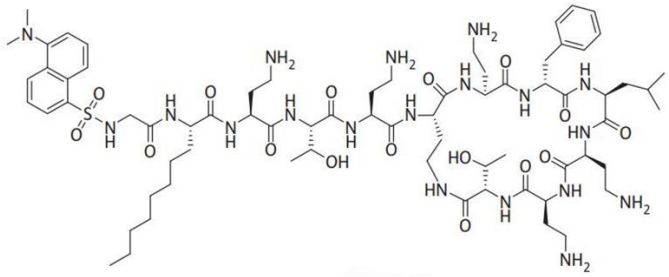

Fig. 7 Structure of MIPS-9541

Cellular uptake of MIPS-9541 was initiated at room temperature using pH 5 PBS with 5 mM glucose. The concentration of MIPS-9541 was 20 μM. Cell fluorescence accumulation was measured using a Tecan Safire II microplate reader (Life Technologies) at an excitation wavelength of 350 nm and an emission wavelength of 518 nm. The uptake of MIPS-9541 was normalized to the fluorescence intensity per 100 mg of protein in each well. The background counts of cells transfected with vector pCI were subtracted from all uptake counts. The data were presented as the mean ± SEM. The experiments were independently conducted three times with three replicates for each condition.

2.7 Transporter kinetic study

Km and Vmax of the mutants with moderately reduced activity in the uptake of ^{3}H-GS and MIPS-9541 were assessed. [^{3}H] Gly-sar uptake was conducted within the concentration range of 0-100 μM; and that of MIPS-9541 is in the range of 0-50 μM (pH 5). . The uptake time was 4 minutes. The kinetic parameters were estimated using GraphPad prism 7.0 software. .

2.8 Statistics

The statistical differences between two normally distributed data sets were analysed using the student's t-test (Statistical Package for the Social Sciences). Differences in the transport function of PepT2 were evaluated with or without treatments by one-way analysis of variance (ANOVA) followed by Dunnett's multiple comparison test. The data are presented as mean ± standard error of the mean (SEM), with statistical significance being determined at a significance level of less than 0.05 for the transport function and inhibition experiments.

Mutation of residue 79
GAA→GCA

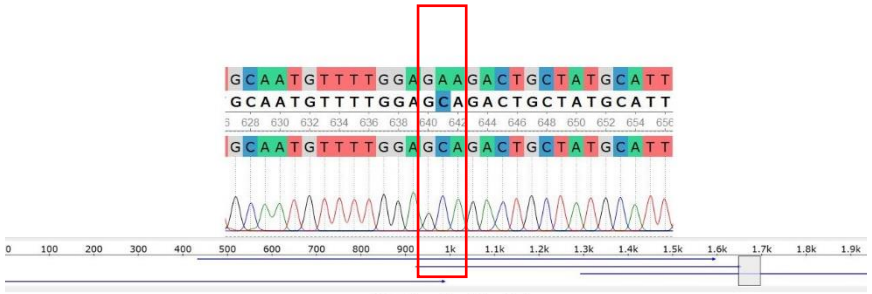

Mutation of residue 214
GAA→GCA

Mutation of residue 208
GAT→GCT

Mutation of residue 215
GAC→GCC

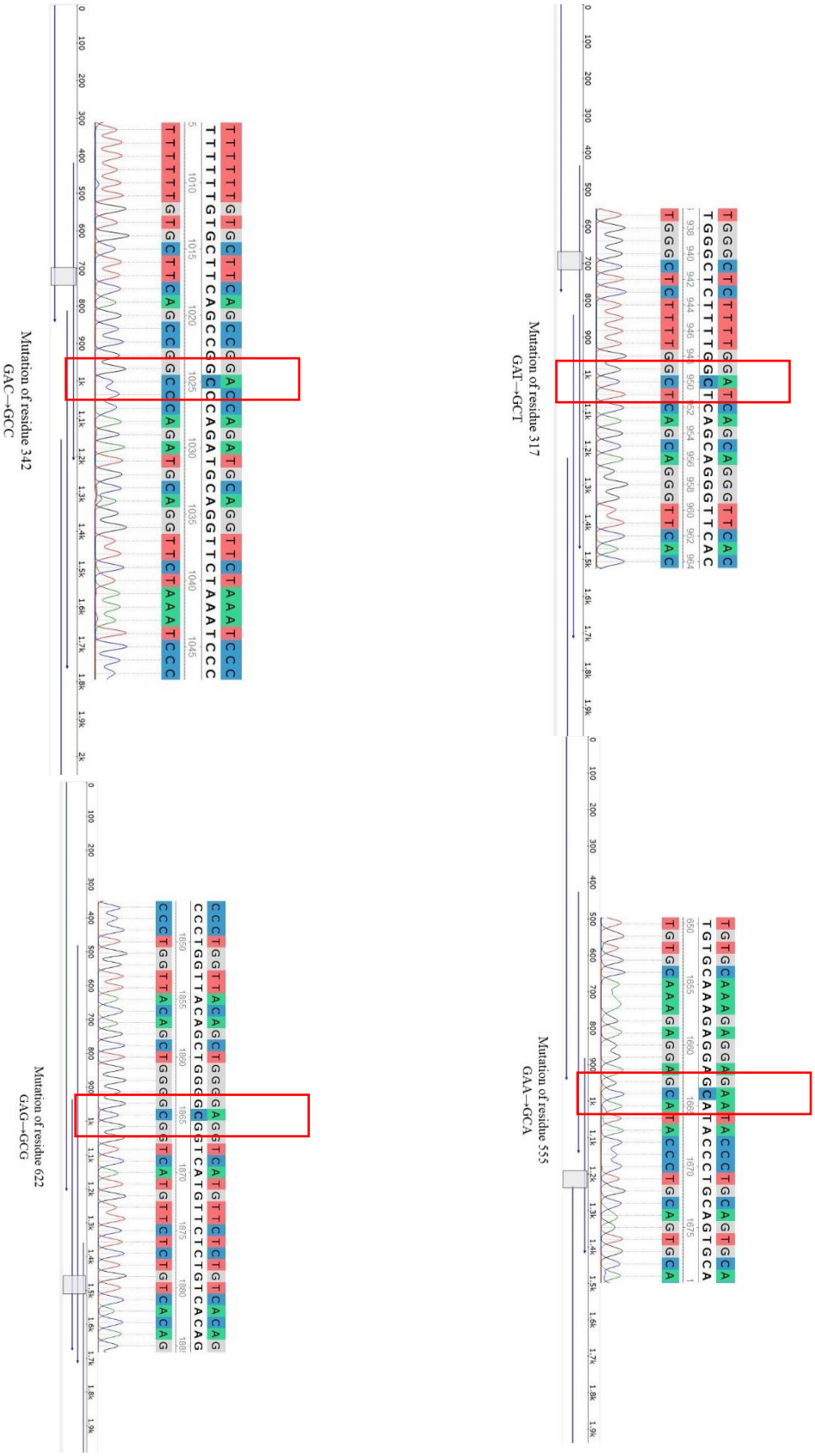

Fig. 8 The human oligopeptide transporter plasmid DNA sequence containing single residue mutation.

	PCR steps					
		25 cycles				
Mutagenesis site	Initial denaturation	Denaturation	Annealing	Extension	Final extension	Storage
79	98°C	98°C	65°C	72°C	72°C	4°C
208			65°C			
214			65°C			
215			65°C			
317			65°C			
342			65°C			
555			65°C			
622			65°C			
79CF			63°C			
Time	30s	10s	15s	210s	10min	

Table 1. PCR condition of mutant construction

Oligo Name	MW	Tm°	GC%	Volume and Concentration	Sequence (5' - 3')
hp2 E79A forward	12712	76.2	41.4	941µl/20µM	ATATAGATGTGGAGGTATCTGCAJTCCAGTGCAGGAAATAC
hp2 E79A reverse	12494	76.2	41.4	812µl/20µM	GTATTTCCTGCACTGGAATGCAGATACCTCCACATCTATAT
hp2 D208A forward	10636	81.8	51.4	867µl/20µM	CTCCAAAACATTGCACAGCTCCTCTCAGCATGGGT
hp2 D208A reverse	10867	81.8	51.4	800µl/20µM	ACCCATGCTGAGAGGAGCTGTGCAATGTTTTGGAG
hp2 E214A forward	11286	81.7	45.9	816µl/20µM	GCCAATGCATAGCAGTCTGCTCCAAAACATTGCACAT
hp2 E214A reverse	11451	81.7	45.9	825µl/20µM	ATGTGCAATGTTTTGGAGCAGACTGCTATGCATTGGC
hp2 D215A forward	11922	81.4	43.5	1079µl/20µM	AAAAGCCAATGCATAGCAGGCTTCTCCAAAACATTGCAC
hp2 D215A reverse	12050	81.4	43.5	870µl/20µM	GTGCAATGTTTTGGAGAAGCCTGCTATGCATTGGCTTTT
hp2 D317A forward	9508	82.4	58	875µl/20µM	CCCGAGAAAACCGAGTCGTCCCAAGTGC
hp2 D317A reverse	9525	82.4	58	722µl/20µM	GGGCTCTTTTTGGCTCAGCAGGGTTCACG
hp2 D342A froward	8913	84	62	875µl/20µM	GAACCTGCATCTGGGCCGGCTGAAGCACA
hp2 D342A reverse	8886	84	62	804µl/20µM	TGTGCTTCAGCCGGCCCAGATGCAGGTTC
hp2 E555A forward	10112	80.1	54.5	1012µl/20µM	GTGCACTGCAGGGTATGCTCCTCTTTGCACAGT
hp2 E555A reverse	10154	80.1	54.5	943µl/20µM	ACTGTGCAAAGAGGAGCATACCCTGCAGTGCAC
hp2 E622A forward	12126	75.7	43.5	748µl/20µM	GACAGAGAACATGACCGCCCCAGCTGTAACCAG
hp2 E622A reverse	11846	75.7	43.5	948µl/20µM	CTGGTTACAGCTGGGCCGGTCATGTTCTCTGTC

Table 2. Primer sequence of hPepT2 mutant constrcution

Results

3. Results

3.1 Molecular characterization of hPepT2 and its mutants in overexpressing HEK293 cells.

As indicated in the previous research, HEK293 cells exhibited minimal endogenous transporter expression and were minimally affected by transfection [105]. These characteristics render HEK293 cells particularly advantageous for the over-expression of SLC transporters and widely employed in vitro transporter study. The mutant hPepT2 transporter genes were transfected into HEK293 cells in the current investigation.

Fig 9 illustrates the differential accumulation of [^{3}H]-labelled Gly-sar in HEK293 cells overexpressing hPepT2 and its mutants. The 208 mutant demonstrated a significantly increased transporter function than hPepT2. In contrast, mutations at positions 214, 215, 317, 342, and 622 decreased the influx of ^{3}H-Gly-Sar.

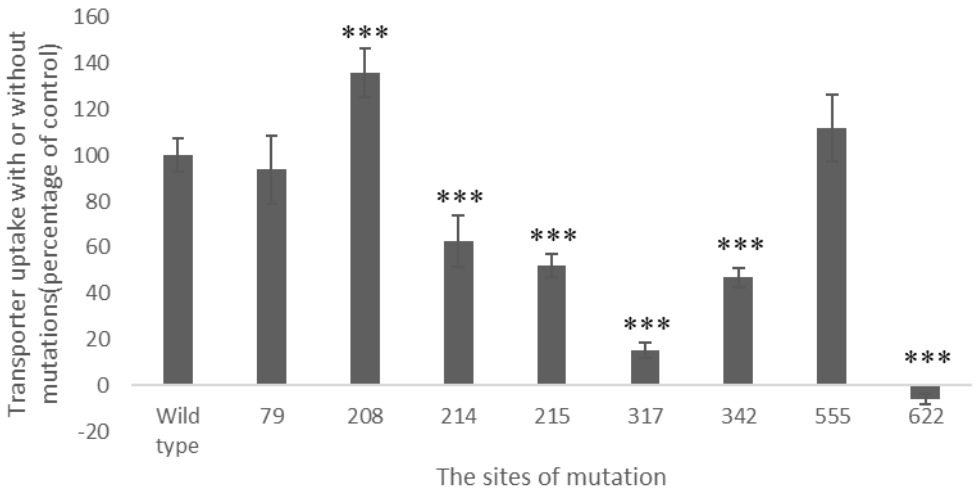

Fig. 9 Uptake of H3-GS in HEK293 cells transfected with hPepT2 and its mutants. The experiments were conducted independently on three occasions with three replicates. Consequently, a total of nine replicates were performed, ensuring the robustness and reliability of the findings. The data values are presented as the mean accompanied by the standard error of the mean (SEM). Significant difference from the control: *** $p < 0.01$

3.2 The kinetic analysis of hPepT2 and its mutants-mediated Gly-sar uptake in HEK293 cells

This study aimed to investigate whether there were any alterations in the substrate-transporter binding affinity or the maximal velocity of the transporter mutants. To accomplish this, kinetic analysis was performed using varying concentrations of ^{3}H-Gly-Sar (ranging from 0 to 100 μM) during a 4-minute incubation period. Specifically, the mutant forms of hPepT2 DNA were examined, namely 208, 214, 215, and 342.

Based on the data presented in Figure 10 and Table 3, the Km values of hPepT2 and the mutants assessed were comparable. The Km values for hPepT2, 208, 214, 215, and 342 were determined as: hPepT2 (39.64 ± 3.004 μM), 208 (42.00 ± 3.519 μM), 214 (44.37 ± 3.365 μM), 215 (42.59 ± 7.909 μM), and 342 (49.66 ± 5.908 μM).

However, it is noteworthy that mutant 208 exhibited the highest Vmax [187.8 ± 6.948 pmol/(μg4min)], while the order of decreasing Vmax values was observed as: hPepT2 [(148.8 ± 4.916 pmol/(μg4min)], 214 [100.4 ± 3.403 pmol/(μg4min)], 342 [88.26 ± 5.178 pmol/(μg4min)], and 215 [65.84 ± 5.857 pmol/(μg*4min)].

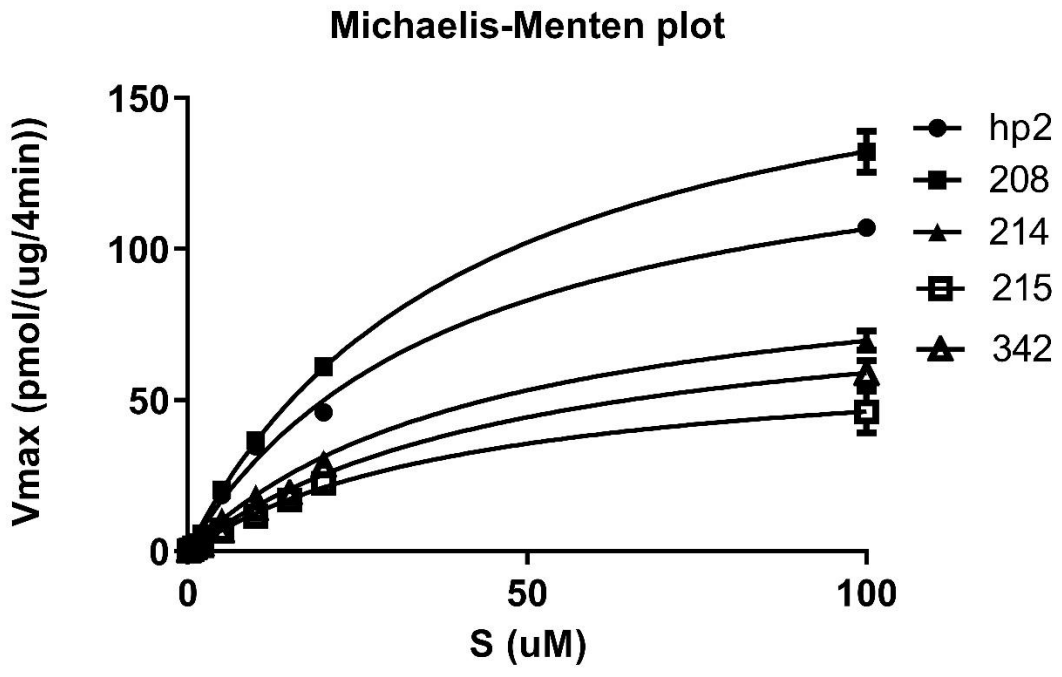

Fig. 10 Kinetic analysis of hPepT2 and its mutants-mediated 3H-Gly-sar uptake.

The cellular uptake of ^{3}H-Gly-sar was evaluated in HEK293 cells that were transfected either with four mutant hPepT2 DNAs or with the vector alone. Kinetic parameters pertaining to the uptake of ^{3}H-Gly-sar were determined in HEK293 cells that were transiently transfected with either mutant 208, 214, 215, 342, or the vector. The uptake assessment was conducted using various concentrations of ^{3}H-Gly-sar, ranging from 0.2 to 100 mM, while accounting for the background uptake observed in the vector-transfected control cells. The GraphPad Prism 9.5.1 software was employed to calculate the Km and Vmax values associated with the uptake of ^{3}H-Gly-sar. The experiments were conducted independently on three occasions with three replicates.

Construct	Km (μM)	Vmax [pmol/(μg/4min)]
hPepT2	39.64 ± 3.004	148.8 ± 4.916
208	42.00 ± 3.519	187.8 ± 6.948
214	44.37 ± 3.365	100.4 ± 3.403*
215	42.59 ± 7.909	65.84 ± 5.857***
342	49.66 ± 5.908	88.26 ± 5.178***

Table 3. The summary of Km and Vmax uptake values of ^{3}H-Gly-sar. Significant difference from the control: *P<0.5, *** p< 0.01

3.3 The cellular uptake of polymyxin B via hPepT2 and its mutants in HEK293 cells

In the previous study [106], it was demonstrated that MIPS-9541, a novel fluorescent probe, effectively preserves the antibacterial and apoptotic properties of polymyxins. This probe was developed by selectively modifying the core scaffold of polymyxin B with a dansyl fluorophore, making it a representative model for the chemical and pharmacological characteristics of polymyxins [103]. Our previous study showed that MIPS-9541 significantly inhibited PepT2-mediated substrate uptake. The calculated IC50 value was determined to be 15.9 ± 1.5 μM [36]. This inhibitory potency was similar to colistin and polymyxin B [104, 107]. Conversely, CMS, an inactive prodrug of colistin known for its diminished nephrotoxicity, exhibited only moderate interaction with this transporter.

And the kinetic analysis conducted in the previous study provided an estimated Km value of 74.9 ± 12.6 μM for the binding affinity between MIPS-9541 and PepT2 [36]. This finding indicates that MIPS-9541 exhibits a strong substrate affinity towards PepT2, as the Km value is comparable to that of the PepT2 prototype substrate, Gly-Sar, which has a Km value of approximately 70 μM [108].

Similar to the characterization process of the different mutant hPepT2 plasmid DNA, the mutant DNA constructs were introduced into HEK 293 cells, resulting in their overexpression. Subsequently, these cells were incubated for 10 minutes at 37 ℃ in pH

5 phosphate-buffered saline (PBS) supplemented with 5 mM glucose and 20 μM MIPS-9541. However, it is worth noting that except mutations at positions 317 and 342, Fig 11 illustrates the differential accumulation of all other mutant hPepT2 DNA constructs exhibited a significant decrease in MIPS-9541 uptake. Furthermore, none of the mutations displayed a higher transporter function in comparison to the wild type hPepT2.

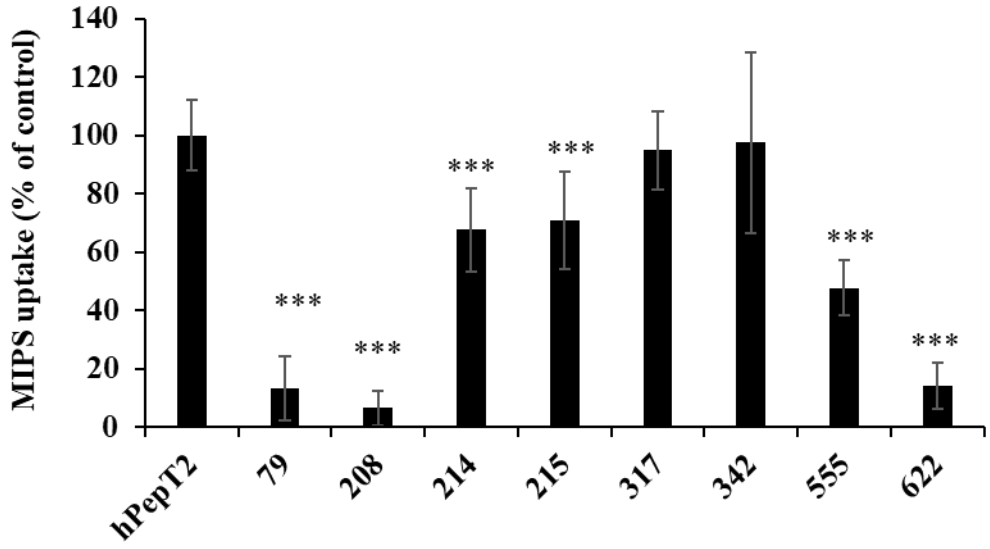

Fig. 11 Uptake of MIPS-9541 in HEK293 cells transfected with hPepT2 and its eight mutants.

Accumulation of MIPS-9541 in HEK293 cells overexpressing relative mutant DNA. The experiments were conducted independently on three occasions with three replicates. Consequently, a total of nine replicates were performed, ensuring the robustness and reliability of the findings. The data values are presented as the mean accompanied by the standard error of the mean (SEM). Significant difference from the control: *** $p < 0.01$

3.4 The kinetic analysis of hPepT2 and its mutants-mediated polymyxin B uptake in HEK293 cells

Although the Km values for each mutant DNA have been previously determined, it is necessary to re-evaluate the Km value for the uptake of polymyxins. This research assessed the Km values for three mutant DNA variants, namely 214, 215, and 555. Based on the data presented in Figure 12 and Table 4, the Km and Vmax values for mutant 214 exhibited minimal differences compared to the wild type [Km: 38.13 ± 12.93μM, Vmax: 3457 ± 671.0 pmol/(μg/4min)]. However, for mutant 215 and 555, the Km and Vmax values were approximately two-fold [Km: 96.56 ± 20.85μM, Vmax: 8610 ± 1363.0 pmol/(μg/4min)] and a half [Km: 26.66 ± 6.99 μM, Vmax: 2376 ± 320.8 pmol/(μg/4min)], respectively, compared to that of the wild type.

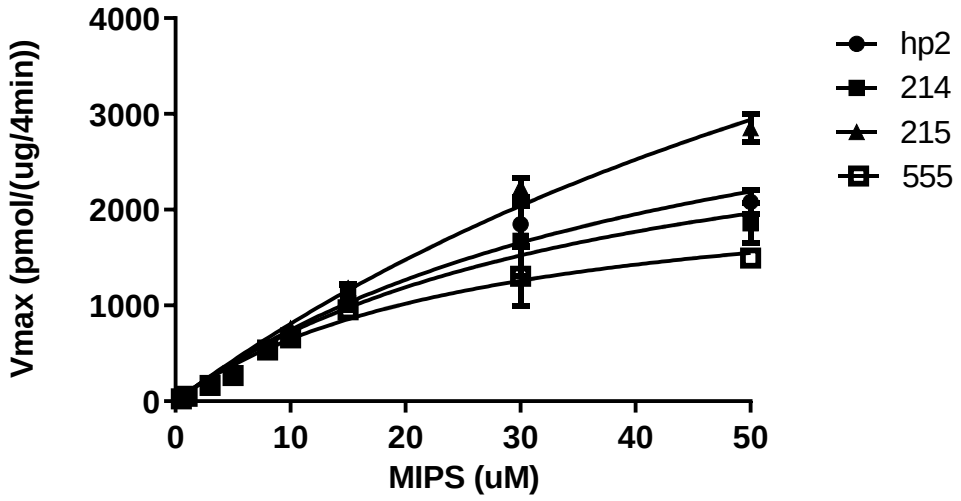

Fig. 12 The cellular uptake of MIPS-9541 was evaluated in HEK293 cells that were transfected either with hPepT2 and its mutants.

Kinetic parameters pertaining to the uptake of MIPS-9541 were determined in HEK293 cells that were transiently transfected with either mutant 214, 215, 555, or the vector. The uptake assessment was conducted using various concentrations of MIPS-9541, ranging from 0.5 to 50 μM, while accounting for the background uptake observed in the vector-transfected control cells. The GraphPad Prism 9.5.1 software was employed to calculate the Km and Vmax values associated with the uptake of MIPS-9541. The experiments were conducted independently on three occasions with three replicates.

Construct	Km (μM)	Vmax [pmol/(μg/4min)]
hPepT2	47.11 ± 11.89	4252 ± 652.9
214	38.13 ± 12.93	3457 ± 671.0
215	96.56 ± 20.85*	8610 ± 1363.0*
555	26.66 ± 6.99	2376 ± 320.8*

Table 4. The summary of Km and Vmax values of uptake of MIPS-9541. Significant difference from the control: *P<0.05.

3.5 hPepT2 protein expression

To evaluate the protein expression of hPepT2 and its mutants, it is imperative to evaluate the total cell and plasma membrane expression of the mutant hPepT2 in HEK 293 cells. Although the uptake of mutants has already been tested, assessing the protein

expression on the cell membrane will provide further insights into the functionality of the mutants in comparison to the wild type.

At present, it remains inconclusive whether the impaired function of hPepT2 mutants are resulted from the altered expression of hPepT2 at cell membrane. It may also be a consequence of changed transporter turn-over rate.

Based on Figure 13, no specific band has been observed between the total cell lysate obtained from cells transfected with hPepT2 or vector. This indicated that the hPepT2 primary antibody used may not be valid. Consequently, a strategic decision was made to test the protein expression in cells overexpressing hPepT2 with C-terminal Flag tag (hPepT2-c-Flag). The specific sequence of this C-terminal Flag tag is Asp-Tyr-Lys-Asp-Asp-Asp-Asp-Lys. Subsequent Western blot analysis was performed, and the result in Figure 14 demonstrated a specific band in hPepT2-c-Flag overexpressing cells.

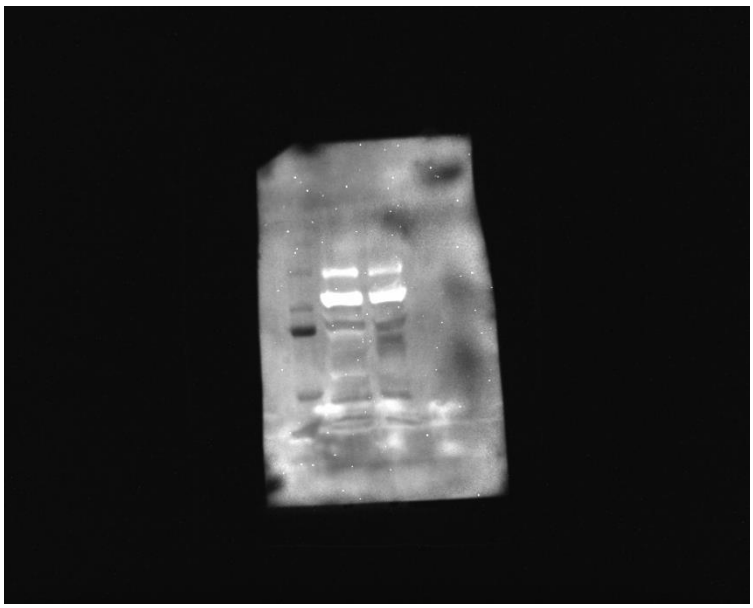

Fig. 13 Protein expression of hPepT2 with anti-PepT2 antibody incubation.

The hPepT2 -expressing cell lysate was on the left, while the vector-transfected cell lysate was on the right. The ImageQuant LAS 500 system was utilized to capture the Western blot image.

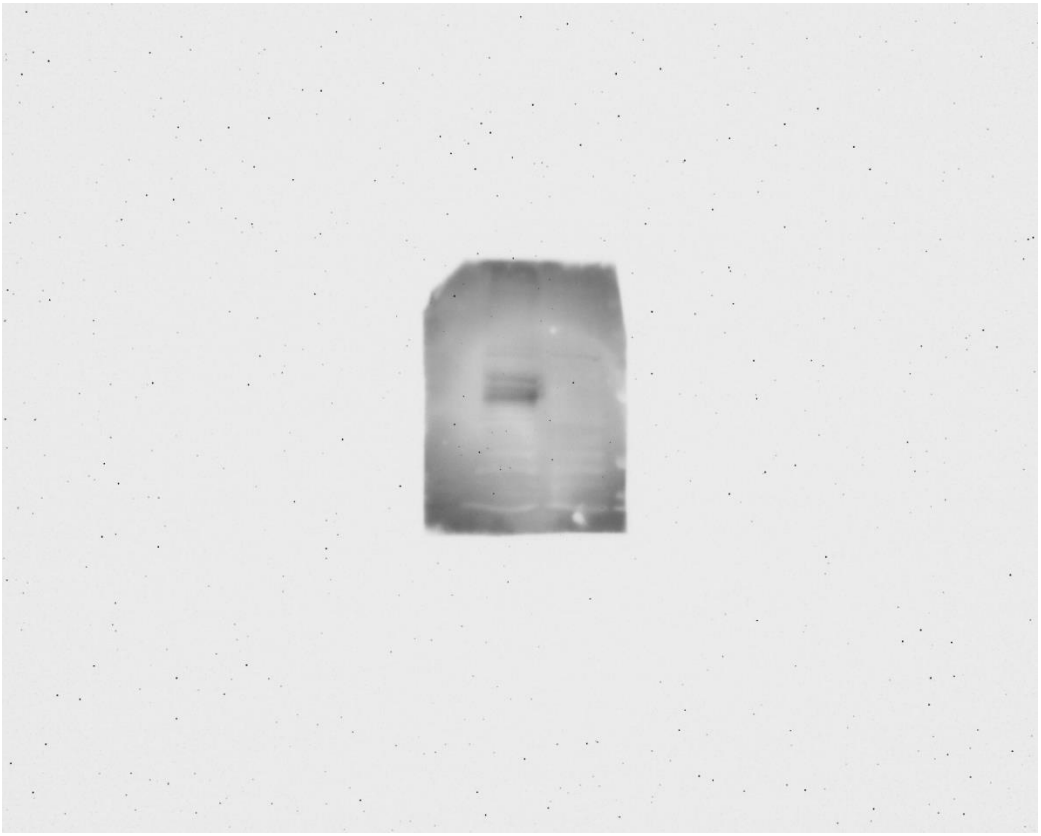

Fig. 14 Protein expression of hPepT2-c-Flag with anti-Flag antibody incubation.

The hPepT2-c-Flag expressing cell lysate was on the left, while the vector-transfected cell lysate was on the right. The ImageQuant LAS 500 system was utilized to capture the Western blot image.

Discussion

4. Discussion

The predominant challenge in the current clinical utilization of polymyxin remains unmanageable and severe nephrotoxicity. Due to its potential side effects and limited clinical data, a safe and reliable dosage has yet to be established. Renal toxicity primarily arises from the reabsorption mechanism in the kidneys, with the transport of polymyxin being facilitated by the human oligopeptide transporter 2 (hPepT2). PepT2, functioning as a transporter with high affinity but low capacity, has the ability to transport over 400 dipeptides and 8,000 tripeptides. These peptides are composed of the 20 essential L-α-amino acids as well as the majority of D-enantiomers [66].

In prior investigations, we have ascertained the interplay between polymyxin and hPepT2. However, the precise correlation between specific pharmacophores of polymyxin and hPepT2 remains uncertain. This research aimed to identify the crucial residues of hPepT2 that are important for its recognition of polymyxins. Ultimately, these findings will be utilized to formulate a comprehensive structural-activity relationship model that guides the chemical modification of polymyxins in the future.

It is uncertain of the molecular mechanisms underpinning the reduced transport activity of 622 mutant. Further investigation is required to evaluate the protein expression of 622 mutant at plasma membrane and in total cell lysis, which may help to explain the functional impairment of this mutant. However, the uptake of MIPS-9541 in other

mutant variants showed varying degrees of reduction, while Gly-sar uptake was significantly higher in mutant 208 compared to the wild type. Noteworthy, the mutant 317 and 342 exhibited a comparable level of MIPS-9541 uptake, while the uptake of ^{3}H-Gly-sar mediated by this mutant was below 40% and 50%.

Mutants 79 and 208 showed similar or higher uptake of ^{3}H-Gly-sar compared to hPepT2, indicating that their transport function for this substrate is maintained or enhanced. However, their uptake of MIPS-9541 was only 20% of the wild-type level, suggesting a significant reduction in their ability to transport MIPS-9541.

On the other hand, mutants 214 displayed lower uptake of ^{3}H-Gly-sar and MIPS-9541 compared to the wild type, indicating a decreased transport capacity for these substrates. Mutant 215 exhibits a varying degree of reduction in uptake for both substrates, whereas mutant 555 only shows a decrease in uptake for MIPS-9541.

Km and Vmax are indicative of the substrate-transporter binding affinity and/or the maximal velocity of the transporter mutants that have undergone alterations. Based on the kinetic results of ^{3}H-Gly-sar, we can conclude that there is no significant difference in Km values of mutants 208, 214, 215, and 342 compared to that of the wild type, indicating comparable substrate affinity to Gly-sar. However, the Vmax of mutant 208 is higher than that of the wild type, while that of the other mutants are lower than the wild type.

Regarding the Km and Vmax of MIPS-9541, mutant 215 exhibited significantly lower affinity than the wild type and an increased Vmax, while mutant 214 displayed a similar affinity and a slighter decreased Vmax to the wild type. On the other hand, mutant 555 showed a comparable affinity to the wild type but a reduced maximal velocity of transporter.

The changed Vmax may be a result of altered transporter protein expression or a change in the turnover rate of PepTs. Further studies will be required to clarify the detailed mechanism associated with such observation.

To mitigate the renal toxicity of polymyxin, it is essential to identify the critical binding sites between polymyxin and hPepT2. Specifically, sites that maintain normal transport function for other substrates while significantly reducing binding with polymyxin are particularly interesting for further investigation. Based on the results obtained, mutant 79, 208, 215, 555, and 622 are promising residues for polymyxin uptake to be further explored. Among them, mutant 215, which exhibits unchanged affinity for ^{3}H-Gly-sar but a significant decrease in affinity for MIPS-9541, is the most plausible candidate for the targeted mutation site in this research.

Further analysis is needed to determine the underlying mechanisms behind the altered substrate uptake and affinity observed in these mutants. This will aid in identifying the

critical binding sites and understanding their roles in reducing the nephrotoxicity of polymyxin.

Conclusion and future studies

5. Conclusion and future studies

This study is the first to explore the structure-activity relationship between polymyxin and hPepT2, to form the basis for chemically modifying polymyxins with reduced nephrotoxicity.

The future research will require constructing new mutants with C-terminal Flag tagged hPepT2 in favour of assessing their protein expression. The mutants exhibiting changed protein expression may hold greater value for further investigation.

The emergence of antibiotic-resistant bacteria has raised a critical demand for effective alternative antibiotics. To develop polymyxins that maintain reasonable antibacterial properties but with minimal nephrotoxicity would be a solution to the health threats. By reducing the renal toxicity associated with polymyxins, patients would benefit from improved therapeutic outcomes and a lower risk of adverse effects overall. This innovation could promote the clinical applications of polymyxins, enabling their use in a broader range of patients suffering from MDR infections.

In conclusion, the development of safer polymyxins holds immense clinical significance. It may revolutionize the treatment of multidrug-resistant bacterial infections in patients contributing to the global effort to combat antibiotic resistance.

References

References

1. Alanis AJ. Resistance to antibiotics: are we in the post-antibiotic era? Arch Med Res. 2005;36(6):697-705.

2. Evelina T. Global Priority List of Antibiotic-Resistant Bacteria to Guide Research, Discovery, and Development. South Africa: Infection Control Africa Network; 2017 2017-02-28.

3. Antibiotic resistance: World Health Organization; 2020 [https://www.who.int/news-room/fact-sheets/detail/antibiotic-resistance].

4. Chaib F. New report calls for urgent action to avert antimicrobial resistance crisis: World Health organization 2019 [https://www.who.int/news/item/29-04-2019-new-report-calls-for-urgent-action-to-avert-antimicrobial-resistance-crisis].

5. Cooper MA, Shlaes D. Fix the antibiotics pipeline. Nature. 2011;472(7341):32.

6. Subramaniam G, Girish M. Antibiotic Resistance - A Cause for Reemergence of Infections. Indian J Pediatr. 2020;87(11):937-44.

7. Li J, Nation RL, Turnidge JD, Milne RW, Coulthard K, Rayner CR, et al. Colistin: the re-emerging antibiotic for multidrug-resistant Gram-negative bacterial infections. Lancet Infect Dis. 2006;6(9):589-601.

8. Landman D, Georgescu C, Martin DA, Quale J. Polymyxins revisited. Clin Microbiol Rev. 2008;21(3):449-65.

9. Velkov T, Thompson PE, Nation RL, Li J. Structure−Activity Relationships of Polymyxin Antibiotics. Journal of Medicinal Chemistry. 2010;53(5):1898-916.

10. Hall-Stoodley L, Costerton JW, Stoodley P. Bacterial biofilms: from the Natural environment to infectious diseases. Nature Reviews Microbiology. 2004;2(2):95-108.

11. Høiby N, Krogh Johansen H, Moser C, Song Z, Ciofu O, Kharazmi A. Pseudomonas aeruginosa and the in vitro and in vivo biofilm mode of growth. Microbes Infect. 2001;3(1):23-35.

12. Fux CA, Costerton JW, Stewart PS, Stoodley P. Survival strategies of infectious biofilms. Trends Microbiol. 2005;13(1):34-40.

13. Pamp SJ, Gjermansen M, Johansen HK, Tolker-Nielsen T. Tolerance to the antimicrobial peptide colistin in Pseudomonas aeruginosa biofilms is linked to metabolically active cells, and depends on the pmr and mexAB-oprM genes. Mol Microbiol. 2008;68(1):223-40.

14. Hengzhuang W, Wu H, Ciofu O, Song Z, Høiby N. In vivo pharmacokinetics/pharmacodynamics of colistin and imipenem in Pseudomonas aeruginosa biofilm infection. Antimicrob Agents Chemother. 2012;56(5):2683-90.

15. Lora-Tamayo J, Murillo O, Bergen PJ, Nation RL, Poudyal A, Luo X, et al. Activity of colistin combined with doripenem at clinically relevant concentrations against multidrug-resistant Pseudomonas aeruginosa in an in vitro dynamic biofilm model. J Antimicrob Chemother. 2014;69(9):2434-42.

16. Bergen PJ, Forrest A, Bulitta JB, Tsuji BT, Sidjabat HE, Paterson DL, et al. Clinically relevant plasma concentrations of colistin in combination with imipenem enhance pharmacodynamic activity against multidrug-resistant Pseudomonas aeruginosa at multiple inocula. Antimicrob Agents Chemother. 2011;55(11):5134-42.

17. Herrmann G, Yang L, Wu H, Song Z, Wang H, Høiby N, et al. Colistin-tobramycin combinations are superior to monotherapy concerning the killing of biofilm Pseudomonas aeruginosa. J Infect Dis. 2010;202(10):1585-92.

18. Papagelopoulos PJ, Mavrogenis AF, Giannitsioti E, Kikilas A, Kanellakopoulou K, Soucacos PN. Management of a multidrug-resistant Pseudomonas aeruginosa infected total knee arthroplasty using colistin. A case report and review of the literature. J Arthroplasty. 2007;22(3):457-63.

19. Landman D, Georgescu C, Martin DA, Quale J. Polymyxins Revisited. Clinical Microbiology Reviews. 2008;21(3):449-65.

20. Nation RL, Velkov T, Li J. Colistin and Polymyxin B: Peas in a Pod, or Chalk and Cheese? Clinical Infectious Diseases. 2014;59(1):88-94.

21. Yuan Z, Tam VH. Polymyxin B: a new strategy for multidrug-resistant Gram-negative organisms. Expert Opin Investig Drugs. 2008;17(5):661-8.

22. Hancock RE. Antibacterial peptides and the outer membranes of gram-negative bacilli. J Med Microbiol. 1997;46(1):1-3.

23. Ofek I, Cohen S, Rahmani R, Kabha K, Tamarkin D, Herzig Y, et al. Antibacterial synergism of polymyxin B nonapeptide and hydrophobic antibiotics in experimental gram-negative infections in mice. Antimicrob Agents Chemother. 1994;38(2):374-7.

24. Hancock RE, Lehrer R. Cationic peptides: a new source of antibiotics. Trends Biotechnol. 1998;16(2):82-8.

25. Otvos L, Jr. Antibacterial peptides and proteins with multiple cellular targets. J Pept Sci. 2005;11(11):697-706.

26. Kohanski MA, Dwyer DJ, Hayete B, Lawrence CA, Collins JJ. A common mechanism of cellular death induced by bactericidal antibiotics. Cell. 2007;130(5):797-810.

27. Storm DR, Rosenthal KS, Swanson PE. Polymyxin and related peptide antibiotics. Annu Rev Biochem. 1977;46:723-63.

28. Sabnis A, Hagart KL, Klöckner A, Becce M, Evans LE, Furniss RCD, et al. Colistin kills bacteria by targeting lipopolysaccharide in the cytoplasmic membrane. Elife. 2021;10.

29. Sivanesan S, Roberts K, Wang J, Chea SE, Thompson PE, Li J, et al. Pharmacokinetics of the Individual Major Components of Polymyxin B and Colistin in Rats. J Nat Prod. 2017;80(1):225-9.

30. Li J, Milne RW, Nation RL, Turnidge JD, Smeaton TC, Coulthard K. Use of high-performance liquid chromatography to study the pharmacokinetics of colistin sulfate in rats following intravenous administration. Antimicrob Agents Chemother. 2003;47(5):1766-70.

31. Yun B, Azad MA, Wang J, Nation RL, Thompson PE, Roberts KD, et al. Imaging the distribution of polymyxins in the kidney. J Antimicrob Chemother. 2015;70(3):827-9.

32. Azad MA, Roberts KD, Yu HH, Liu B, Schofield AV, James SA, et al. Significant accumulation of polymyxin in single renal tubular cells: a medicinal chemistry and triple correlative microscopy approach. Anal Chem. 2015;87(3):1590-5.

33. Eshbach ML, Weisz OA. Receptor-Mediated Endocytosis in the Proximal Tubule. Annu Rev Physiol. 2017;79:425-48.

34. Manchandani P, Zhou J, Babic JT, Ledesma KR, Truong LD, Tam VH. Role of Renal Drug Exposure in Polymyxin B-Induced Nephrotoxicity. Antimicrob Agents Chemother. 2017;61(4).

35. Suzuki T, Yamaguchi H, Ogura J, Kobayashi M, Yamada T, Iseki K. Megalin contributes to kidney accumulation and nephrotoxicity of colistin. Antimicrob Agents Chemother. 2013;57(12):6319-24.

36. Lu X, Chan T, Xu C, Zhu L, Zhou QT, Roberts KD, et al. Human oligopeptide transporter 2 (PEPT2) mediates cellular uptake of polymyxins. J Antimicrob Chemother. 2016;71(2):403-12.

37. E B. Fundamentals of protein structure and function. 2015(Switzerland: Springer International Publishing).

38. Daniel H, Rubio-Aliaga I. An update on renal peptide transporters. Am J Physiol Renal Physiol. 2003;284(5):F885-92.

39. Ganapathy, Leibach FH. Is intestinal peptide transport energized by a proton gradient? Am J Physiol. 1985;249(2 Pt 1):G153-60.

40. Ganapathy V, Leibach FH. Carrier-mediated reabsorption of small peptides in renal proximal tubule. Am J Physiol. 1986;251(6 Pt 2):F945-53.

41. Fei YJ, Kanai Y, Nussberger S, Ganapathy V, Leibach FH, Romero MF, et al. Expression cloning of a mammalian proton-coupled oligopeptide transporter. Nature. 1994;368(6471):563-6.

42. Martinez Molledo M, Quistgaard EM, Flayhan A, Pieprzyk J, Low C. Multispecific Substrate Recognition in a Proton-Dependent Oligopeptide Transporter. Structure. 2018;26(3):467-76 e4.

43. Groneberg DA, Döring F, Eynott PR, Fischer A, Daniel H. Intestinal peptide transport: ex vivo uptake studies and localization of peptide carrier PEPT1. Am J Physiol Gastrointest Liver Physiol. 2001;281(3):G697-704.

44. Rühl A, Hoppe S, Frey I, Daniel H, Schemann M. Functional expression of the peptide transporter PEPT2 in the mammalian enteric nervous system. J Comp Neurol. 2005;490(1):1-11.

45. Bhardwaj RK, Herrera-Ruiz D, Eltoukhy N, Saad M, Knipp GT. The functional evaluation of human peptide/histidine transporter 1 (hPHT1) in transiently transfected COS-7 cells. Eur J Pharm Sci. 2006;27(5):533-42.

46. Zhao D, Lu K. Substrates of the human oligopeptide transporter hPEPT2. BioScience Trends. 2015;9(4):207-13.

47. Smith DE, Pavlova A, Berger UV, Hediger MA, Yang T, Huang YG, et al. Tubular localization and tissue distribution of peptide transporters in rat kidney. Pharm Res. 1998;15(8):1244-9.

48. Shen H, Smith DE, Keep RF, Brosius FC, 3rd. Immunolocalization of the proton-coupled oligopeptide transporter PEPT2 in developing rat brain. Mol Pharm. 2004;1(4):248-56.

49. Kramer W, Girbig F, Gutjahr U, Kleemann HW, Leipe I, Urbach H, et al. Interaction of renin inhibitors with the intestinal uptake system for oligopeptides and beta-lactam antibiotics. Biochim Biophys Acta. 1990;1027(1):25-30.

50. Friedman DI, Amidon GL. Passive and carrier-mediated intestinal absorption components of two angiotensin converting enzyme (ACE) inhibitor prodrugs in rats: enalapril and fosinopril. Pharm Res. 1989;6(12):1043-7.

51. Friedman DI, Amidon GL. Intestinal absorption mechanism of dipeptide angiotensin converting enzyme inhibitors of the lysyl-proline type: lisinopril and SQ 29,852. J Pharm Sci. 1989;78(12):995-8.

52. Bretschneider B, Brandsch M, Neubert R. Intestinal transport of beta-lactam antibiotics: analysis of the affinity at the H+/peptide symporter (PEPT1), the uptake into Caco-2 cell monolayers and the transepithelial flux. Pharm Res. 1999;16(1):55-61.

53. Walter E, Kissel T, Reers M, Dickneite G, Hoffmann D, Stüber W. Transepithelial transport properties of peptidomimetic thrombin inhibitors in monolayers of a human intestinal cell line (Caco-2) and their correlation to in vivo data. Pharm Res. 1995;12(3):360-5.

54. de Vrueh RL, Smith PL, Lee CP. Transport of L-valine-acyclovir via the oligopeptide transporter in the human intestinal cell line, Caco-2. J Pharmacol Exp Ther. 1998;286(3):1166-70.

55. Balimane PV, Tamai I, Guo A, Nakanishi T, Kitada H, Leibach FH, et al. Direct evidence for peptide transporter (PepT1)-mediated uptake of a nonpeptide prodrug, valacyclovir. Biochem Biophys Res Commun. 1998;250(2):246-51.

56. Wenzel U, Thwaites DT, Daniel H. Stereoselective uptake of beta-lactam antibiotics by the intestinal peptide transporter. Br J Pharmacol. 1995;116(7):3021-7.

57. Brandsch M, Thunecke F, Küllertz G, Schutkowski M, Fischer G, Neubert K. Evidence for the absolute conformational specificity of the intestinal H+/peptide symporter, PEPT1. J Biol Chem. 1998;273(7):3861-4.

58. Sugawara M, Huang W, Fei YJ, Leibach FH, Ganapathy V, Ganapathy ME. Transport of valganciclovir, a ganciclovir prodrug, via peptide transporters PEPT1 and PEPT2. J Pharm Sci. 2000;89(6):781-9.

59. Döring F, Walter J, Will J, Föcking M, Boll M, Amasheh S, et al. Delta-aminolevulinic acid transport by intestinal and renal peptide transporters and its physiological and clinical implications. J Clin Invest. 1998;101(12):2761-7.

60. Brandsch M, Knütter I, Thunecke F, Hartrodt B, Born I, Börner V, et al. Decisive structural determinants for the interaction of proline derivatives with the intestinal H+/peptide symporter. Eur J Biochem. 1999;266(2):502-8.

61. Meredith D, Temple CS, Guha N, Sword CJ, Boyd CA, Collier ID, et al. Modified amino acids and peptides as substrates for the intestinal peptide transporter PepT1. Eur J Biochem. 2000;267(12):3723-8.

62. Abe H, Satoh M, Miyauchi S, Shuto S, Matsuda A, Kamo N. Conjugation of dipeptide to fluorescent dyes enhances its affinity for a dipeptide transporter (PEPT1) in human intestinal Caco-2 cells. Bioconjug Chem. 1999;10(1):24-31.

63. Knütter I, Theis S, Hartrodt B, Born I, Brandsch M, Daniel H, et al. A novel inhibitor of the mammalian peptide transporter PEPT1. Biochemistry. 2001;40(14):4454-8.

64. Niida A, Tomita K, Mizumoto M, Tanigaki H, Terada T, Oishi S, et al. Unequivocal synthesis of (Z)-alkene and (E)-fluoroalkene dipeptide isosteres to probe structural requirements of the peptide transporter PEPT1. Org Lett. 2006;8(4):613-6.

65. Brandsch M. Transport of L-proline, L-proline-containing peptides and related drugs at mammalian epithelial cell membranes. Amino Acids. 2006;31(2):119-36.

66. Wang M, Zhang X, Zhao H, Wang Q, Pan Y. Comparative analysis of vertebrate PEPT1 and PEPT2 genes. Genetica. 2010;138(6):587-99.

67. Rubio-Aliaga I, Daniel H. Mammalian peptide transporters as targets for drug delivery. Trends Pharmacol Sci. 2002;23(9):434-40.

68. Verrey F, Singer D, Ramadan T, Vuille-dit-Bille RN, Mariotta L, Camargo SM. Kidney amino acid transport. Pflugers Arch. 2009;458(1):53-60.

69. Daniel H, Adibi SA. Transport of beta-lactam antibiotics in kidney brush border membrane. Determinants of their affinity for the oligopeptide/H+ symporter. J Clin Invest. 1993;92(5):2215-23.

70. Akarawut W, Lin CJ, Smith DE. Noncompetitive inhibition of glycylsarcosine transport by quinapril in rabbit renal brush border membrane vesicles: effect on high-affinity peptide transporter. J Pharmacol Exp Ther. 1998;287(2):684-90.

71. Terada T, Saito H, Inui K. Interaction of beta-lactam antibiotics with histidine residue of rat H+/peptide cotransporters, PEPT1 and PEPT2. J Biol Chem. 1998;273(10):5582-5.

72. Geissler S, Zwarg M, Knütter I, Markwardt F, Brandsch M. The bioactive dipeptide anserine is transported by human proton-coupled peptide transporters. Febs j. 2010;277(3):790-5.

73. Biegel A, Knütter I, Hartrodt B, Gebauer S, Theis S, Luckner P, et al. The renal type H+/peptide symporter PEPT2: structure-affinity relationships. Amino Acids. 2006;31(2):137-56.

74. Groneberg DA, Fischer A, Chung KF, Daniel H. Molecular mechanisms of pulmonary peptidomimetic drug and peptide transport. Am J Respir Cell Mol Biol. 2004;30(3):251-60.

75. Knütter I, Hartrodt B, Tóth G, Keresztes A, Kottra G, Mrestani-Klaus C, et al. Synthesis and characterization of a new and radiolabeled high-affinity substrate for H+/peptide cotransporters. Febs j. 2007;274(22):5905-14.

76. Smith DE, Clemencon B, Hediger MA. Proton-coupled oligopeptide transporter family SLC15: physiological, pharmacological and pathological implications. Mol Aspects Med. 2013;34(2-3):323-36.

77. Xu J, Zeug A, Riederer B, Yeruva S, Griesbeck O, Daniel H, et al. Calcium-sensing receptor regulates intestinal dipeptide absorption via Ca(2+) signaling and IK(Ca) activation. Physiol Rep. 2020;8(1):e14337.

78. Fei YJ, Liu JC, Fujita T, Liang R, Ganapathy V, Leibach FH. Identification of a potential substrate binding domain in the mammalian peptide transporters PEPT1 and PEPT2 using PEPT1-PEPT2 and PEPT2-PEPT1 chimeras. Biochem Biophys Res Commun. 1998;246(1):39-44.

79. Terada T, Irie M, Okuda M, Inui K. Genetic variant Arg57His in human H+/peptide cotransporter 2 causes a complete loss of transport function. Biochem Biophys Res Commun. 2004;316(2):416-20.

80. Döring F, Dorn D, Bachfischer U, Amasheh S, Herget M, Daniel H. Functional analysis of a chimeric mammalian peptide transporter derived from the intestinal and renal isoforms. J Physiol. 1996;497 (Pt 3)(Pt 3):773-9.

81. Terada T, Saito H, Sawada K, Hashimoto Y, Inui K. N-terminal halves of rat H+/peptide transporters are responsible for their substrate recognition. Pharm Res. 2000;17(1):15-20.

82. Döring F, Martini C, Walter J, Daniel H. Importance of a small N-terminal region in mammalian peptide transporters for substrate affinity and function. J Membr Biol. 2002;186(2):55-62.

83. Chen XZ, Steel A, Hediger MA. Functional roles of histidine and tyrosine residues in the H(+)-peptide transporter PepT1. Biochem Biophys Res Commun. 2000;272(3):726-30.

84. Bolger MB, Haworth IS, Yeung AK, Ann D, von Grafenstein H, Hamm-Alvarez S, et al. Structure, function, and molecular modeling approaches to the study of the intestinal dipeptide transporter PepT1. J Pharm Sci. 1998;87(11):1286-91.

85. Sala-Rabanal M, Loo DD, Hirayama BA, Wright EM. Molecular mechanism of dipeptide and drug transport by the human renal H+/oligopeptide cotransporter hPEPT2. Am J Physiol Renal Physiol. 2008;294(6):F1422-32.

86. Kukuruzinska MA, Lennon K. Protein N-glycosylation: molecular genetics and functional significance. Crit Rev Oral Biol Med. 1998;9(4):415-48.

87. Dorn M, Jaehme M, Weiwad M, Markwardt F, Rudolph R, Brandsch M, et al. The role of N-glycosylation in transport function and surface targeting of the human solute carrier PAT1. FEBS Lett. 2009;583(10):1631-6.

88. Hoover RS, Poch E, Monroy A, Vázquez N, Nishio T, Gamba G, et al. N-Glycosylation at two sites critically alters thiazide binding and activity of the rat thiazide-sensitive Na(+):Cl(-) cotransporter. J Am Soc Nephrol. 2003;14(2):271-82.

89. Stelzl T, Baranov T, Geillinger KE, Kottra G, Daniel H. Effect of N-glycosylation on the transport activity of the peptide transporter PEPT1. Am J Physiol Gastrointest Liver Physiol. 2016;310(2):G128-41.

90. Chan T, Lu X, Shams T, Zhu L, Murray M, Zhou F. The Role of N-Glycosylation in Maintaining the Transporter Activity and Expression of Human Oligopeptide Transporter 1. Mol Pharm. 2016;13(10):3449-56.

91. Stelzl T, Geillinger-Kastle KE, Stolz J, Daniel H. Glycans in the intestinal peptide transporter PEPT1 contribute to function and protect from proteolysis. Am J Physiol Gastrointest Liver Physiol. 2017;312(6):G580-G91.

92. Newstead S, Drew D, Cameron AD, Postis VL, Xia X, Fowler PW, et al. Crystal structure of a prokaryotic homologue of the mammalian oligopeptide-proton symporters, PepT1 and PepT2. Embo j. 2011;30(2):417-26.

93. Solcan N, Kwok J, Fowler PW, Cameron AD, Drew D, Iwata S, et al. Alternating access mechanism in the POT family of oligopeptide transporters. EMBO J. 2012;31(16):3411-21.

94. Doki S, Kato HE, Solcan N, Iwaki M, Koyama M, Hattori M, et al. Structural basis for dynamic mechanism of proton-coupled symport by the peptide transporter POT. Proc Natl Acad Sci U S A. 2013;110(28):11343-8.

95. Guettou F, Quistgaard EM, Trésaugues L, Moberg P, Jegerschöld C, Zhu L, et al. Structural insights into substrate recognition in proton-dependent oligopeptide transporters. EMBO Rep. 2013;14(9):804-10.

96. Boggavarapu R, Jeckelmann JM, Harder D, Ucurum Z, Fotiadis D. Role of electrostatic interactions for ligand recognition and specificity of peptide transporters. BMC Biol. 2015;13:58.

97. Parker JL, Li C, Brinth A, Wang Z, Vogeley L, Solcan N, et al. Proton movement and coupling in the POT family of peptide transporters. Proc Natl Acad Sci U S A. 2017;114(50):13182-7.

98. Lyons JA, Parker JL, Solcan N, Brinth A, Li D, Shah ST, et al. Structural basis for polyspecificity in the POT family of proton-coupled oligopeptide transporters. EMBO Rep. 2014;15(8):886-93.

99. Martinez Molledo M, Quistgaard EM, Low C. Tripeptide binding in a proton-dependent oligopeptide transporter. FEBS Lett. 2018;592(19):3239-47.

100. Beale JH, Parker JL, Samsudin F, Barrett AL, Senan A, Bird LE, et al. Crystal Structures of the Extracellular Domain from PepT1 and PepT2 Provide Novel Insights into Mammalian Peptide Transport. Structure. 2015;23(10):1889-99.

101. Killer M, Wald J, Pieprzyk J, Marlovits TC, Löw C. Structural snapshots of human PepT1 and PepT2 reveal mechanistic insights into substrate and drug transport across epithelial membranes. Sci Adv. 2021;7(45):eabk3259.

102. Quistgaard EM, Martinez Molledo M, Löw C. Structure determination of a major facilitator peptide transporter: Inward facing PepTSt from Streptococcus thermophilus crystallized in space group P3121. PLoS One. 2017;12(3):e0173126.

103. Azad MA, Yun B, Roberts KD, Nation RL, Thompson PE, Velkov T, et al. Measuring polymyxin uptake by renal tubular cells: is BODIPY-polymyxin B an appropriate probe? Antimicrob Agents Chemother. 2014;58(10):6337-8.

104. Spapen H, Jacobs R, Van Gorp V, Troubleyn J, Honoré PM. Renal and neurological side effects of colistin in critically ill patients. Ann Intensive Care. 2011;1(1):14.

105. Ahlin G, Hilgendorf C, Karlsson J, Szigyarto CA, Uhlén M, Artursson P. Endogenous gene and protein expression of drug-transporting proteins in cell lines routinely used in drug discovery programs. Drug Metab Dispos. 2009;37(12):2275-83.

106. Deris ZZ, Swarbrick JD, Roberts KD, Azad MA, Akter J, Horne AS, et al. Probing the penetration of antimicrobial polymyxin lipopeptides into gram-negative bacteria. Bioconjug Chem. 2014;25(4):750-60.

107. Bergen PJ, Li J, Rayner CR, Nation RL. Colistin methanesulfonate is an inactive prodrug of colistin against Pseudomonas aeruginosa. Antimicrob Agents Chemother. 2006;50(6):1953-8.

108. Ocheltree SM, Shen H, Hu Y, Xiang J, Keep RF, Smith DE. Role of PEPT2 in the choroid plexus uptake of glycylsarcosine and 5-aminolevulinic acid: studies in wild-type and null mice. Pharm Res. 2004;21(9):1680-5.